

15115

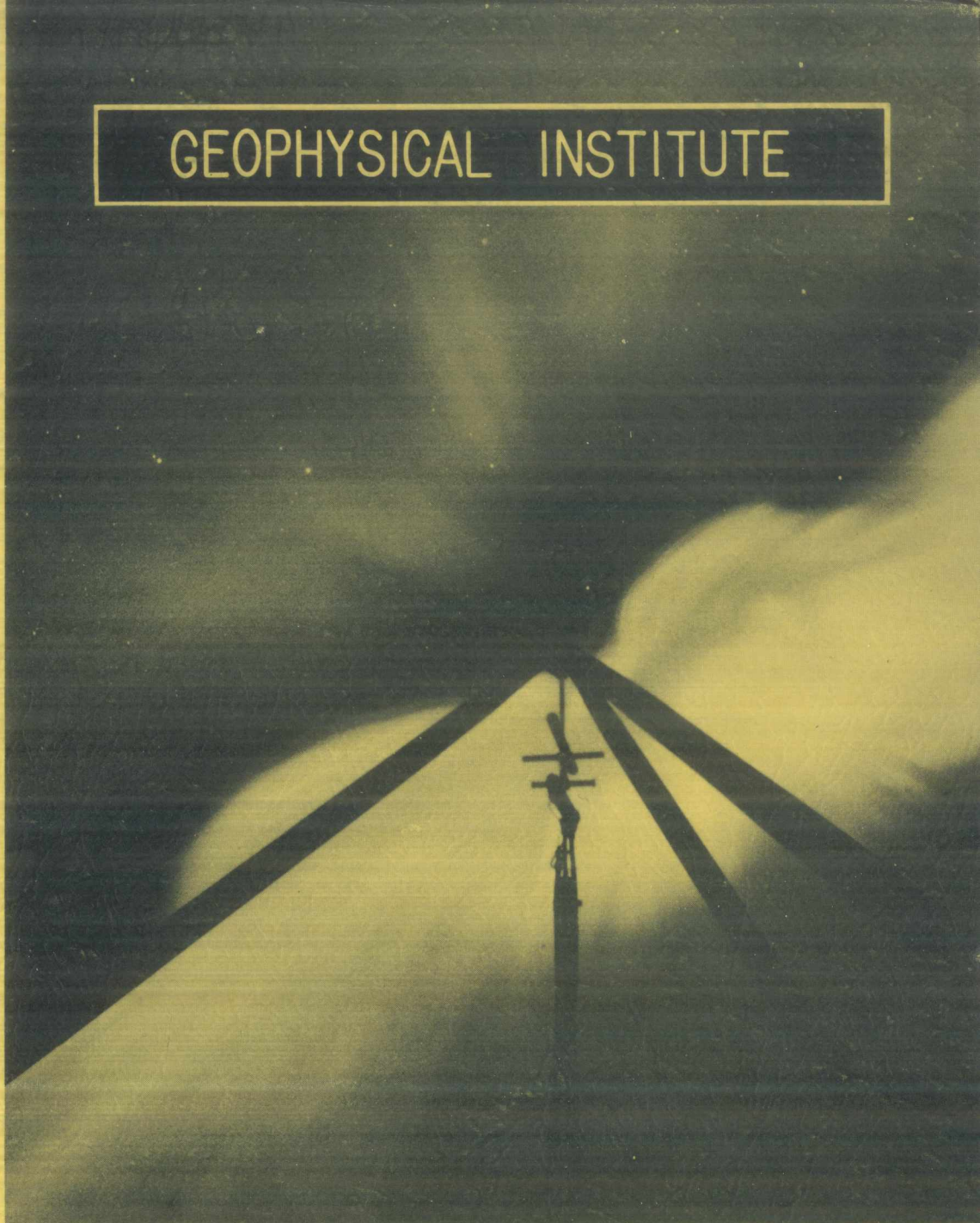
GEOPHYSICAL INSTITUTE

AFCRL-194

UNIVERSITY
OF ALASKA

COLLEGE
ALASKA

UAG-R115



AN HF SWEEP FREQUENCY STUDY OF THE ARCTIC IONOSPHERE

GEOPHYSICAL INSTITUTE
UNIVERSITY OF ALASKA

by

Howard F. Bates

Scientific Report No. 1
Air Force Research Contracts
AF 19(604)-1859 and AF 19(604)-5574
April 1961

ASSISTANT DIRECTOR'S OFFICE

Electronics Research Directorate
Air Force Cambridge Research Laboratories

GEOPHYSICAL INSTITUTE
of the
UNIVERSITY OF ALASKA

Scientific Report No. 1

AN HF SWEEP FREQUENCY STUDY OF THE ARCTIC IONOSPHERE

by

Howard F. Bates

April, 1961

The research reported in this document has been sponsored by the Electronics Research Directorate of the Air Force Cambridge Research Laboratories, Office of Aerospace Research (USAF), Bedford, Mass. under Contracts No. AF 19(604)-1859 and AF 19(604)-5574.

Approved by:

C. T. Elvey
C. T. Elvey
Director

"Requests for additional copies by Agencies of the Department of Defense, their contractors, and other Government agencies should be directed to the:

ARMED SERVICES TECHNICAL INFORMATION AGENCY
ARLINGTON HALL STATION
ARLINGTON 12, VIRGINIA

Department of Defense contractors must be established for ASTIA services or have their 'need-to-know' certified by the cognizant military agency of their project or contract".

"All other persons and organizations should apply to the:

U.S. DEPARTMENT OF COMMERCE
OFFICE OF TECHNICAL SERVICES
WASHINGTON 25, D.C."

ERRATA

Page 2. Chapter numbers listed in last paragraph should run from 1 through 5 rather than 2 through 6.

Page 9. Equation 2.2 should read,

$$\rho c = \left(\frac{h_o}{h_o + y_m} \right)^{1/2} \equiv K$$

TABLE OF CONTENTS

	Page
INTRODUCTION	1
CHAPTER 1.	
HISTORICAL REVIEW OF THE MID-LATITUDE HF SCATTER RESEARCH	3
CHAPTER 2.	
HF SCATTER RESEARCH AT THE GEOPHYSICAL INSTITUTE	15
A. Equipment	16
B. Typical sweep frequency records	23
CHAPTER 3.	
THE IONOSPHERIC SCATTER PROBLEM	28
CHAPTER 4.	
MODELS FOR IF AND THE CONSTANT RANGE ECHOES	32
CHAPTER 5.	
APPLICATIONS OF THESE ECHOES TO IONOSPHERIC RESEARCH	38
CHAPTER 6.	
RECOMMENDATIONS FOR FURTHER RESEARCH	52
CHAPTER 7.	
CONCLUSIONS	54
ACKNOWLEDGEMENTS	56
BIBLIOGRAPHY	57

LIST OF FIGURES

Figure

1. Possible backscatter mode types.
2. Equivalent and actual path geometry.
3. Block diagram of NBS Model C4 ionosonde.
4. Clipper-mixer amplifier diagram.
5. Examples of 2F groundscatter.
6. Particular examples of 1F, 2F, and constant range traces.
7. Line drawing of Figure 6.
8. Typical 1F echoes.
9. Simultaneously occurring 1F and 2F echoes.
10. Constant range echoes.
11. Possible 3F backscatter echoes.
12. Cusped, oblique echoes.
13. Cusped, oblique echoes.
14. Slant Es echoes.
15. Typical 1F trace.
16. Calculated 1F trace.
17. Example of slant Es echo.
18. High resolution vertical incidence trace for Figure 18.
19. Typical constant range trace.
20. Line drawing of Figure 19.
21. Calculated 1F and constant range traces.
22. Geometry for constant range trace calculation.
23. Typical examples of 1F trace.

LIST OF FIGURES (CONT'D.)

Figure

24. Line drawing of Figure 23A.
25. Morning sequence, 16 November 1958.
26. Morning sequence, 20 December 1958.
27. Afternoon sequence, 20 December 1958.
28. Slant Es sequence, 28 December 1958.
29. College 41 Mc/s radar record, 28 December 1958.

Table 1. - Page 48

ABSTRACT

Observations made during 1958 and 1959 using a sweep frequency, HF, oblique sounder located at College, Alaska, are discussed, and selected groups of echoes are illustrated. Groundscatter is the predominant echo type observed on mid-latitude backscatter records, but this is not true in the high latitudes. The majority of the scatter echoes from soundings toward geomagnetic north were direct F region scatter of two main types - 1F and constant range echoes. These same echo types were observed from the E region during magnetic disturbances (the slant Es echo corresponds to the 1F echo). These echoes were centered about geomagnetic north on swept azimuth soundings and were produced by scatter near the oblique reflection point in the ionosphere. Thus, we conclude that the echoes were caused by scatter from irregularities aligned along the geomagnetic field.

The 1F echo branches off the first order vertical incidence F region trace and increases linearly in range with frequency. It is produced by scattered energy which is least-time focused. The scatterers are essentially randomly distributed within large regions called clouds in the F region. The height of the irregularities producing the 1F echo can be computed if the vertical incidence traces are clear; heights between 200 and 350 km have been found by this technique, indicating that electron density irregularities are not confined only to the lower ionosphere. From the regularity of occurrence of the 1F echo, it is highly probable that the irregularities extend throughout much of the F region.

The constant range echo is produced by energy scattered from the field-aligned surface of a cloud of irregularities. The soundings were

made to the north so the clouds producing the observed constant range echo extended east and west.

The 1F and the constant range echoes are useful research tools because they indicate the amount of cloudiness present in the F region. During the summer day, the F region is relatively free of clouds, while during the winter night, it is quite overcast. The cloud size and distribution depend primarily upon the zenith angle of the sun, the smaller the zenith angle, the smaller and fewer the clouds.

Geomagnetic effects do not appear to influence the behavior or the F region clouds, although this point is somewhat uncertain. The E region clouds which produced the slant Es echo were definitely correlated with geomagnetic activity but not to solar radiation. There appeared to be no connection between the causes of the E and the F region direct scatter echoes even though they were propagated by the same general mechanisms.

This study raised several new problems whose explanations might contribute greatly to ionospheric research. The sweep frequency sounding technique is a good method, but the system sensitivity must be raised greatly over that of the present equipment if meaningful results are to be obtained.

INTRODUCTION

At present, radio methods are the most productive and easily applied techniques for routine ionospheric measurements. Of the various radio techniques which have been devised, the ionosonde is now the most widely used. Using this method, one sends out a short pulse of radio frequency energy and usually, but not necessarily, observes the scattered or reflected echoes at the transmitting site. The echoes are displayed by recording their equivalent range (time of propagation multiplied by the speed of light) as a function of time, frequency, or direction. If the origin and the mode of propagation of a particular echo can be identified, one or several characteristics of the ionospheric region being sounded can be determined. For example, vertical incidence echoes can be utilized to determine the height and the free-electron content of the various ionospheric layers. With the pulsed sounder technique the major problem is the proper identification of the propagation mode involved. Unless this can be done, no information about the ionosphere can be derived from the observed echoes.

This study is primarily concerned with the identification of two types of direct scatter from the F region and how these echoes can be used. Although direct scatter from the upper ionosphere has been observed in the mid-latitudes, it is a rare occurrence. However, at high latitudes the situation is quite different as direct scatter echoes of two types are regularly observed at College, Alaska.

Some of the echoes propagated via the ionosphere have proven to be directly useful to communications. The vertical incidence echo noted above is one example. Groundscatter, discussed at length in Chapter 2,

is another; from it we can obtain within a matter of a few minutes the HF propagation characteristics between any points we choose on the earth. Other examples are forward scatter echoes from meteor trails and from other E region irregularities which have led to two important types of long distance communications.

The primary use of some of the other observed scatter modes is as a research tool rather than as a direct benefit to communications. The E and F region direct scatter modes to be discussed are examples of this. They do not appear to be very useful either for point to point communications or for predicting propagation conditions, but they do yield valuable information about the spatial and the temporal variations of the irregularities in the ionospheric electron density.

The organization of this study is as follows. Chapter 2 is an historical survey of mid-latitude scatter research (little or no work has been published previously on high latitude HF backscatter). Chapter 3 outlines the sweep frequency program at the Geophysical Institute and contains some typical records obtained during the two years of observation. In Chapter 4 we discuss some of the theoretical aspects of scatter from electron density irregularities. Chapter 5 is devoted to the theoretical models to explain two of the frequently observed scatter echoes, and Chapter 6 outlines some of the applications of these echoes to ionospheric research.

HISTORICAL REVIEW OF THE MID-LATITUDE SCATTER RESEARCH

In this study we shall discuss various HF propagation modes involving the F region, so some sort of uniform notation is necessary from the beginning. Of the many scatter paths that are theoretically possible, only those illustrated in Figure 1 need be considered. These are all single-scatter modes so propagation in either direction is equally probable. Refraction has been ignored in the schematic representation. All references to types of propagation paths in the rest of this study will be to those shown in Figure 1.

Scatter echoes in the HF band were first observed shortly after long distance communications were found to be possible. The echoes were apparently discovered independently in 1926 by two workers, Taylor (Taylor and Young 1928) and Mögel (Dieminger 1951). During this period much of the HF communications research was concentrated on round-the-world echoes in the hope that they would provide a method of determining the height of the Kennelly-Heaviside layer.

Taylor in the United States monitored various European and United States, Morse code stations and noticed that occasionally the characters were greatly elongated when the receiver was not in the skip zone, or that signals were sometimes received when the receiver was inside the skip zone. This latter observation led to speculation about the correctness of the skip zone theory, but in 1929 Taylor and Young were able to show conclusively that the signals received inside the skip zone were scatter, and that the theory was valid. By using highly directional antennas, Taylor and Young determined the azimuthal angle of arrival of the echoes and found that they came from the direction opposite to the

transmitter. They concluded that the echoes were caused by scatter from some point on the propagation path but suggested no theory to explain them.

During this period other workers considered the echoes, and, in light of contemporary knowledge, several novel theories were proposed. Quack and Mogel (1929) noted the regularity in the delay time of the echoes and concluded that they were reflected from a height of 1500 km in the atmosphere. Hoag and Andrew (1928) suggested that the scatter came from the polar ionosphere. They postulated that the height of the ionosphere increased sharply towards the pole, producing a surface like an inverted bowl which trapped and returned the incident energy. They also considered the possibility that the aurora might cause some scatter, and today we know that such is the case.

While there was some additional work and speculation on the scatter, problem in the 1930's, only Eckersley (1932, 1937, 1939, and 1940) made a concerted effort to solve it. Unfortunately, he was biased toward the idea that the majority of the echoes were the result of scatter from E region irregularities (types 2 or 4, Figure 1). In 1939 he showed that the equivalent range as a function of frequency fell on a line tangent to the second-order vertical incidence trace from the F layer but did not recognize the significance of this observation. The scatter problem was not resolved until Dieminger (1951), and Peterson (1951) correctly deduced that this fact held the key to the solution. Eckersley's 1940 paper was quite an extensive attack on the problem.

As World War II progressed, the scatter problem was apparently dropped in favor of more vital communications problems. Some work was published, however, in the early 1940's. Pierce and Mimno (1940)

attempted to explain the scatter echoes by assuming that an increase in the curvature of the ionosphere, caused by traveling disturbances, produced the scatter. Edwards and Jansky (1941) tried to measure the angle of arrival of the echoes as well as the delay time, but the measurements were not accurate enough to determine the origin of the echoes. They postulated that some were type 3 scatter from the ground as well as scatter from E region clouds of the form of types 2 and 4, Figure 1.

During the mid and late 1940's the research on the HF scatter problem was renewed and many new workers entered the field. The evidence that the majority of the echoes were type 3 groundscatter increased as the 1950's approached, although Eckersley still clung to the E scatter hypothesis in papers published in 1944 and 1948. Peterson (1949), Gates (1949), Silberstein (1949), and Hartsfield et al (1949) reported that although some E region scatter was observed, groundscatter appeared to be predominant.

The last three papers resulted from a cooperative test between the National Bureau of Standards and the U.S. Navy Electronics Laboratory. A transmitter was installed by the Central Radio Propagation Laboratory of N.B.S. at Sterling, Va., and transponders were located at Alamogordo, N. M., and at San Diego, California. The pulses from Sterling were recorded at the transponder sites, and the transponder pulses and the backscatter echoes were recorded at Sterling. The workers concluded from their data that the majority of the scatter originated on the ground at or near the edge of the skip zone.

During the latter 1940's several workers (e.g. Benner 1949) realized that if the echoes were actually groundscatter, they might be useful for short term predictions of point-to-point propagation conditions. At that

time the leading edge of the backscatter echoes was assumed to be composed of energy scattered from the edge of the skip zone. Therefore, the equivalent range of the echo would give the slant range to the edge of the skip zone, and if one assumed a height of reflection, the ground distance to the edge of the skip zone could be calculated. The frequency used in the sounding was then the maximum frequency (MUF) which would propagate between the transmitter and the calculated point. Thus, to determine the MUF between two given points, one would determine the range of the scatter echoes for a band of frequencies transmitted from one point towards the other. The MUF would be given by the frequency at which the equivalent range of the leading edge of the echo equalled the slant range between the points. The equivalent height of reflection at the midpoint of the path would have to be assumed, but this introduces at most a small error since the height is not critical in the calculation.

The breakthrough on the scatter problem occurred in the early 1950's when Peterson (1951), Dieminger (1951), Abel and Edwards (1951), and Silberstein (1954) proved conclusively that the majority of the mid-latitude echoes originated at the ground. With this discovery the interest in scatter echoes shifted abruptly, and the research was essentially concentrated on two new problems. The first was how well one could predict MUF's from the groundscatter echoes, and the second was the origin of the anomalous or non-groundscatter echoes that were occasionally observed. This study is concerned mostly with the latter problem, but a brief outline of the published work on the communications problem is included for completeness.

Abel and Edwards (1951) reported on several years of experimental work undertaken by Raytheon Manufacturing Company at Waltham, Mass.

Raytheon originally contracted to develop an HF early warning radar for the U.S. Air Force, but the scatter echoes completely masked the wanted radar echoes. In an effort to discover and possibly eliminate the source of the interfering scatter, they set up a high powered pulse transmitter at Waltham, and a series of four transponders at distances of 700, 1000, 1500, and 2000 km across the United States. Four frequencies at approximately 9, 12, 16, and 22 Mc/s were used with highly directional antennas. Several years data showed that at least sixty-five per cent of the scatter occurred at the ground. This work was originally classified so its publication in the open literature was delayed until after the results of other workers were published.

Dieminger (1951) in Germany employed both fixed and sweep frequency transmissions to show that the scatter echoes usually branched off the second order vertical incidence F layer trace. Using this fact and a somewhat qualitative argument, Dieminger showed that such echoes had to originate at the surface of the earth. His paper contains some good sweep frequency groundscatter records.

Work was started at Stanford University on the scatter problem in the latter 1940's. The Stanford group was investigating HF meteor echoes, and the scatter echoes were observed as interference. Although Peterson set up an experimental program for the observation of backscatter echoes using a fixed frequency sounder, his primary contribution consisted in devising a theoretical model for the propagation of the groundscatter echoes. Comparing the results of his theoretical model with the experimental observations, Peterson (1951) concluded that the majority of the long range, mid-latitude scatter echoes were scatter from the ground propagated via the F layer.

Some of the details of Peterson's analysis are needed in later chapters so the theory is briefly outlined below. Consider a plane, horizontally stratified layer having a parabolic electron distribution in the vertical direction. Collisional losses, the geomagnetic field, and the earth's curvature are neglected; ray theory is used throughout. With reference to Figure 2 for the geometry involved, the oblique incidence equivalent path length P' between A and B is (Appleton and Beynon 1940),

$$2.1 \quad P' = \frac{2h_0}{C} + y_m \rho \ln \frac{1 + \rho C}{1 - \rho C}$$

where f is the transmitting frequency

f_c is the critical frequency of the layer

θ is the angle of incidence upon the base of the layer

h_0 is the height of the base of the layer

y_m is the layer half-thickness

$$\rho = \frac{f}{f_c}$$

$$C = \cos \theta$$

Assume first that randomly distributed irregularities, capable of backscattering energy over the path of incidence shown in Figure 2 exist on the surface of the earth. If a pulse of radio frequency energy at a particular frequency is transmitted at all angles of incidence, the leading edge of the echo will be composed of the energy that traverses the path of minimum time. Since the only variable in Equation 2.1 is the angle of incidence (assuming that we are transmitting on a fixed frequency), the path of minimum time is found by setting the derivative of Equation 2.1

with respect to θ equal to zero. If this is done, we find the following.

$$2.2 \quad \rho_c = \left(\frac{y_o}{y_o + h_m} \right)^{1/2} \approx K$$

From Figure 2 we see that the equivalent height of reflection h' for any oblique path is given by

$$2.3 \quad h' = \frac{P'C}{2}$$

Combining Equations 2.1, 2.2, and 2.3, we have the equivalent height of reflection for the least time path h'_m .

$$2.4 \quad h'_m = h_o + \frac{y_m K}{2} \ln \frac{1+K}{1-K}$$

By definition K is a constant, thus, the equivalent height of reflection for the least time path is a constant for all angles of incidence. Combining Equations 2.2 and 2.3, and solving for the equivalent path of minimum time P'_m , we have,

$$2.5 \quad P'_m = \frac{2h'_m}{K f_c} f$$

The equivalent path of minimum time, therefore, increases linearly with frequency. If we define the frequency f_t as the frequency at which the angle of incidence θ is zero, from Equation 2.2 we have,

$$2.6 \quad f_t = K f_c$$

or

$$2.7 \quad P'_m = \frac{2h'_m}{f_t} f$$

Because f_c is the frequency at which the angle of incidence is zero, at this frequency the vertical incidence and the least time oblique incidence paths coincide. Thus, the leading edge of the ground-scatter trace branches off the second order vertical incidence trace and increases linearly with frequency along the line passing through the origin and tangential to the cusp of the vertical incidence trace.

Peterson also showed the existence of a focusing effect which strongly enhances that portion of the echo propagating via the path of least time. He called this effect 'time-delay' or 'least time' focusing and showed that it caused the echo to build up to its peak amplitude within approximately one pulse width. Hence, the leading edge of back-scatter is an accurate measure of the time taken to traverse the path of least time.

Another important result of Peterson's analysis was that the skip zone ray does not follow the path of least time, and, in fact, the two may differ appreciably at frequencies near the critical frequency. Thus, if the echoes are to be used for MUF predictions, some modification of the technique described above is necessary because the sounding frequency for a given equivalent path is no longer the MUF for that particular slant range. Fortunately, however, at frequencies well above the critical frequency ($f > 1.6$) the two paths do not differ appreciably, and the method for obtaining the MUF as described above can be used directly. In the frequency range $f < 1.3$ a serious error is introduced, but this region is usually of little importance as it corresponds to ground distances of less than 800 km.

At this point a short discussion on notation is required. There is as yet no uniformity on the naming of the modes shown in Figure 1.

In this study the following notation is used. The term nF is used for all single scatter propagation modes in which the energy (both incident and scattered) is incident upon the F region n times and undergoes enhancement by the least-time focusing mechanism. Thus, the type 3 groundscatter echo described above is called the 2F echo, but a type 3 echo received from a fixed region such as a mountain range is not a 2F echo. Basically, the nF echo is a weak scatter echo because it is produced by randomly distributed scatterers. Echoes from a discrete region which require no focusing for their observation are termed strong scatter echoes; the latter type are popularly known as 'radar' echoes.

In the early 1950's several careful experiments were performed to determine the accuracy with which one could predict MUF's from 2F groundscatter echoes, although the results of only two were published in the open literature. The two reported were performed by the Radio Physics Laboratory in Canada and by the National Bureau of Standards in the United States. Both groups reported that one could accurately predict MUF's in most cases, although occasional failures were noted.

In 1951 a group at the National Bureau of Standards installed modified sweep frequency ionospheric sounders at Sterling, Va., Batavia, Ohio, and Boulder, Colorado. These equipments were synchronized to sweep together so that each sounder recorded echoes from its own transmissions plus the direct transmissions from each of the other sounders. Vertical incidence sounders were installed at the midpoints of the Sterling-Batavia and the Sterling-Boulder paths. The results of this experiment were summarized in papers by Silberstein (1954), Wieder (1955), and Sulzer (1955). Silberstein's paper contains some excellent sweep frequency 2F groundscatter records which prove Peterson's analysis is

correct. He reported that most of the observed scatter echoes were 2F groundscatter but noted several other types also. Type 3 strong scatter echoes from the Rocky Mountains were identified, and E region of types 2 or 4 were suggested to explain some of the other echoes.

Wieder and Sulzer discussed the results of the oblique transmissions over the 1150 and the 2400 km paths, respectively. They concluded that the MUF's derived from scatter soundings were very close to the actual values, but that the MUF's predicted by the CRPL method from vertical incidence soundings at the midpoint of the respective paths were systematically about five per cent low. Sulzer, in particular, noted cases in which the observed MUF was considerably above the predicted value.

The Radio Physics Laboratory group in Ottawa installed synchronized, sweep frequency, oblique sounders in Ottawa, Ont. and Saskatoon, Sask., and a vertical sounder at approximately the midpoint. Chapman et al (1955) concluded that the predicted MUF's were approximately equal to the observed MUF's with a small but systematic difference. They made an attempt to check reciprocity and found that it held to the level of precision with which they could make their measurements.

In the late 1950's there was much additional work on the problem of predicting MUF's from oblique transmissions. Because this study is mostly concerned with the non-groundscatter echoes observed at high latitudes, we shall pursue the MUF problem no further. The rest of this chapter is devoted to the non-groundscatter echoes observed in the mid-latitudes.

The results of Peterson, Dieminger, Abel and Edwards, and Silberstein showed that the majority of the echoes were groundscatter. They all noted echoes, however, which did not originate at the ground. Silberstein (1954)

in particular, commented on a type of echo whose range versus frequency trace branched off the fundamental vertical incidence trace. He suggested that the echo was either of type 2 or 4. Various non-groundscatter or 'anomalous' echoes were observed only rarely in the mid-latitudes (the rarity of occurrence accounts for the name), but even so, several types of scatter modes were identified, including types 1, 2, and 4.

The radio auroral echo is a type 1 echo which has received close attention in the past ten years. Originally, the auroral echo was thought to be connected with the visual aurora, hence the name, but this connection still has not been entirely determined. The auroral echo was the subject of an extensive IGY program, the results of which are just now being published. A paper (Booker et al 1955) by the Cornell University group gives an excellent review of the work on the problem prior to 1955 and presents a list of the general properties of the echo, sufficient for our purpose. Reviewing the detailed properties is beyond the scope of this treatment so the echo will be discussed only generally and briefly. It is primarily an E region phenomenon even though Peterson et al (1955) reported occasionally observing F region auroral echoes from Stanford University. Most of the research on the problem has been done in the VHF and the UHF portion of the spectrum because of the difficulties inherent in operating in the HF band. One of the primary characteristics (usually termed 'aspect sensitivity') of the echo is that it is observed only from regions of high electron density (the E or the F layers) in which the line of sight and the geomagnetic field intersect perpendicularly. Thus, in the northern hemisphere the auroral echo is observed only to the north and at a preferred range depending upon the geographical location of the observer. For example, at College,

Alaska, the preferred range is approximately 700 km, assuming an E region scattering height of 100 km (Leadabrand et al 1959).

The final paper to be considered in this chapter is the result of an apparently carefully done experiment in which the path of each echo could be determined with a fair degree of precision. McCue (1956) in South Australia set up a system for observing both the elevation angle of arrival and the travel time of the echoes. Using highly directional but fixed antennas and various frequencies just above and below the critical frequency, he found that type 3 groundscatter predominated and that types 1, 2, and 4 were occasionally observed. Although there have been occasional comments in the literature about type 1 direct backscatter from the F region, most workers have dismissed the possibility because of the lack of a satisfactory scattering mechanism at the high altitudes involved. McCue, however, definitely identified such scatter at small zenith angles (less than fifteen degrees generally). Probably the reason that he observed direct scatter only from nearly overhead was because he operated close to the critical frequency; it is shown in Chapter 5 that the commonest type of direct scatter echo observed at College, Alaska, behaves in precisely that manner.

This concludes the historical review of the mid-latitude research on HF backscatter echoes. The anomalous mid-latitude F region echoes occurred so rarely that their observation was at best difficult and time consuming. Thus, while there was some speculation about their origin, the lack of a sufficient amount of data made the determination of the scattering modes involved generally impossible.

CHAPTER 2.

HF SCATTER RESEARCH AT THE GEOPHYSICAL INSTITUTE

At the Geophysical Institute of the University of Alaska the backscatter sounding program was started in 1953 with the installation of a scatter sounder operating on various frequencies between 5 and 15 Mc/s. The first project was the prediction of the optimum frequency for communications between Eielson Air Force Base and one of their weather flights. In spite of some minor difficulties the program was highly successful. For the first month of operation the predictions were approximately ninety per cent correct, according to the initially-skeptical USAF radio operators.

From the first, many echoes were observed which were not groundscatter. In fact, it soon became evident that at high latitudes the 'anomalous' echoes were observed with such great regularity that the term was not strictly applicable, except from an historical standpoint. In the mid-latitudes groundscatter predominated, but at the high latitudes this was not true.

In latter 1955 a scatter sounder on 12.3 Mc/s was installed and operated on a routine basis until 1957. A continuously rotating Yagi antenna was used, sweeping the azimuth once per minute. Even though much useful data was obtained with the fixed frequency equipments, it was quickly recognized that a multi-frequency system would be necessary so a sweep frequency sounder was ordered. It arrived and was installed in 1957, and after being put into automatic operation in April 1958, it operated approximately one-half the time until May 1960. With this equipment two types of direct scatter echoes from the arctic ionosphere were identified, and these echoes are the subject of this study.

A. The Equipment.

The sweep frequency sounder was a considerably modified National Bureau of Standards Model C4 ionospheric recorder (Brown 1959) built by Barker and Williamson, Inc., Bristol, Pa. Figure 3 is the block diagram of the unmodified sounder which is composed of three basic units - a medium-power pulse transmitter, a pulse-receiving and recording system, and a time-base generator.

The operation of the recorder is as follows. Starting at 1.0 Mc/s, pulses of radio frequency energy are transmitted at successively higher frequencies up to the upper limit of 25.0 Mc/s. Between pulses the receiving system receives and records any echoes of the transmitted pulse which exceed the receiver threshold sensitivity. The range of each echo is recorded on film as a function of the transmitting frequency. The transmitter power-amplifiers are all untuned, as is the input stage of the receiver. Tracking between the transmitter and the receiver is achieved by using a common variable frequency to derive both the transmitting frequency and the frequency of the first local oscillator in the receiver. Specific details about the operation of each unit are discussed below.

The time-base generator produces the range-marks, the DC pulses which control the transmitter, and the oscilloscope sweep and gate voltages. It utilizes an accurate 3000 c/s crystal oscillator and derives the various wave forms from the output of that stage by means of frequency-dividing and wave-shaping circuits.

The controlling variable frequency of the equipment is produced by a variable-frequency oscillator (VFO) which sweeps from 31.0 to 56.0 Mc/s. The transmitting frequency is produced by mixing the output of the VFO

with that of the 30.0 Mc/s fixed-frequency oscillator (FFO), and amplifying the difference frequency in the cascaded, pulsed, power amplifiers in the transmitting unit. These amplifiers are all grid-pulsed to ensure that there is no backwave to interfere with the received signals during the time between transmitted pulses. The system is unbalanced up to the final amplifier, which has a balanced, 600 ohm output impedance.

The receiver is a conventional mixer-input, double conversion system, except that all control-grid circuit time constants are less than 100 microseconds. These short time-constants are necessary to prevent excessive grid-blocking in the receiver from energy coupled directly from transmitter to receiver through the antennas and feedlines. (This directly coupled signal is generally referred to as the 'ground pulse'.) The ground pulse is strong and overdrives the receiver amplifiers, causing the control grids of the amplifier tubes to draw grid current. The impedance of the conducting grid is small so the grid circuit capacitance charges quickly. After the ground pulse, the charge on the grid capacitance produces a negative bias on the now non-conducting control grid, preventing tube conduction. Thus, the amplifier cannot operate until the grid circuit capacitance discharges, which, for practical purposes, occurs after four to five time-constants have elapsed. The charging time-constant is controlled by the impedance of the conducting control grid, but the discharging time-constant depends upon the grid-leak circuit time-constant. Thus, the grid-leak time-constant must be approximately one-fourth the time allowable for the amplifier to achieve its full gain after the ground pulse.

The first stage of the receiver is a balanced to unbalanced mixer in which the VFO output is mixed with the receiver input. Because the VFO output and the transmitter output frequencies differ by 30.0 Mc/s, the VFO output and the receiver input likewise differ by 30.0 Mc/s. Thus, we have automatic tracking with this system. The 30.0 Mc/s output of the first intermediate frequency (IF) amplifier is mixed with a 28.6 Mc/s signal from the second local oscillator and the difference is the second IF at 1.4 Mc/s.

After detection of the second IF the received pulse signals are amplified and recorded on film. The recording unit consists of a 35 mm camera which photographs an intensity modulated oscilloscope trace. During the sweep the film runs vertically past the oscilloscope face; the trace on the oscilloscope sweeps horizontally at a constant rate, starting when the recorder begins its sweep. Received echoes blank that portion of each trace in which the echoes occur so the distance between the start of the trace and the leading edge of the blanked portion is an accurate measure of the travel time of the echo. The frequency is determined by the distance from the start of each individual frame.

The above discussion pertains to the originally unmodified recorder, intended primarily for vertical incidence work. For oblique sounding several modifications were necessary to improve the operation of the equipment. Some required the changing of only one or several components in the existing circuits while others required the introduction of additional circuits. The equipment characteristics and the modifications are listed below.

Equipment Characteristics

Frequency range	1 to 25 Mc/s
Pulse repetition frequency	12 pps
Frequency sweep rate	4 Mc/s/min
Frequency sweep time	6 min
Nominal peak power output	5 kw
Pulse width	600 μ s
Time of operation	Every quarter hour
Range displayed	2500 or 3500 km
Rangemarks	100 or 200 km

Modifications

1. The transmitted pulse width was increased from 50 to 600 microseconds. This was accomplished by increasing the timing capacitor in the transmitter-pulse generator.

Past experience had shown that groundscatter is difficult to obtain with medium power pulse widths of less than 500 microseconds. The shorter pulse requires a wider receiver bandwidth for reproduction. Because the received noise power varies with the bandwidth, the wider bandwidth requires a larger signal amplitude for minimum detectability. Another factor is that the shorter pulse contains less energy, thus less energy is available to be scattered back. In the case of groundscatter this is an important consideration. Peterson (1951) showed that for pulses of less than 500 microseconds, increasing the pulse width increases the echo amplitude. Pulse widths of more than one millisecond, however, do not appreciably affect the echo amplitude. Thus, the optimum is in the neighborhood of 500 to 1000 microseconds for groundscatter. In

general, the optimum pulse width is determined by the scattering mechanism involved.

A 600 microsecond pulse was the longest practicable value which could be used with the equipment. The total allowable power dissipated in the final amplifiers was the primary consideration, although the lack of regulation in the high voltage power supply was an important factor.

2. The range-mark frequency was divided by 2 to produce 200 km range-marks instead of the supplied 100 km marks. This made the reduction of the data easier by decreasing the number of range-marks shown on a given record. The width of the range-marks was simultaneously increased so that they would record more prominently. Originally, the range-mark width was adjusted for good reproduction with the 500 and 1000 km sweeps used for vertical incidence sounding, but because sweep lengths of 2500 to 4000 km were used for the oblique sounding, the widening was necessary. The frequency division was accomplished by adding a stage of conventional binary division just after the 3 kc/s crystal standard in the pulse generator unit.

3. Increasing the transmitted pulse width from 50 to 600 microseconds allowed the use of a 2 to 3 kc/s receiver bandwidth instead of the 25 kc/s bandwidth in the original equipment. Reducing the bandwidth of the second IF amplifier was impractical so a third IF amplifier having a 265 kc/s center frequency and a bandwidth of 3 kc/s was constructed and installed after the 1.4 Mc/s second IF amplifier. This produced a substantial increase in the signal-to-noise ratio by decreasing the received noise power.

4. The detected video output of the third IF amplifier was squared, clipped, and limited. The unit which accomplished this, shown

schematically in Figure 4, consisted essentially of alternate cut-off and zero-biased amplifiers. The detected video input was linearly amplified and then applied to the clipping amplifier as a positive-going signal. The clipping amplifier consisted of a cut-off-biased amplifier with a controllable fixed bias so that the clipping level could be adjusted to any chosen value. Ideally, the clipping level was to be set at the top of the average noise level, thus passing any signal exceeding the noise while excluding the average noise. In practice, however, the noise level was not constant so a compromise had to be made on how much noise could be accepted.

Any pulse which passed the clipper was amplified greatly in the succeeding clipping and squaring amplifiers, producing a rectangular pulse of fixed height as the video output. No matter how much a pulse exceeded the clipping level, the height of the output pulse was constant. Thus, weak echoes which just exceeded the noise level would be recorded as strongly as those which exceeded it greatly. Amplitude information was lost by this technique, but the ability to prominently record weak signals was deemed to off-set this disadvantage.

Originally, the range-marks were applied to the grid of the cathode-ray display tube, but because of some initial instability, the range-marks were mixed with the squared video. The video range-mark signal was then capacitively coupled directly to the cathode of the display tube.

5. In order to increase the accuracy in scaling the frequency from the records, the film was run at three times the normal speed. The frequency sweep was made very slowly so this speeding-up of the film actually reduced the effect of interfering signals. In normal operation the sounder swept through the frequency band in fifteen seconds, but

the oblique sweep took six minutes. With the long sweep and the normal film speed the resolution of the system was not sufficient to prevent the overlapping of several adjacent oscilloscope traces. Thus, on the film, closely spaced interference could cover weak echoes in the clear space between the interfering signals.

From April to October 1958 the antenna system was composed of two sloping Vee antennas, one each for receiving and transmitting. The height at the apex was 80 feet, the leg length 300 feet, and the apex angle 55 degrees. The antennas were beamed at 17 degrees geographic, or roughly half-way between the north geomagnetic and geographic poles. The feed system for the antennas was composed of balanced, open-wire, 600 ohm transmission lines. Each leg of the antennas was terminated at the ground end with a 300 ohm resistance. The impedance characteristics with frequency were not measured.

Even though the measurement of antenna patterns is very difficult at HF, several flights along the axis of the antennas were made with a transmitter at various frequencies. The major lobe of the Vees was approximately 30 degrees above the horizon at 6 Mc/s, and the angle decreased to approximately 8 degrees at 24 Mc/s.

From November 1958 to May 1960 the antenna system was composed of two single wire rhombic antennas, one each for receiving and transmitting. The height was 78 feet, the apex angle 70 degrees, and the leg length 200 feet. They were fed by balanced, open-wire, 600 ohm transmission lines and terminated by 600 ohms. The terminating impedance was a highly dissipative, balanced, open-wire, 600 ohm transmission line constructed of Nichrome wire and terminated by a 600 ohm resistance.

By switching the antenna feed and dissipation line connections, the antennas could be beamed at either 5 or 185 degrees geographic bearing. Thus, although observations with the Vees could be made only to the north, with the rhombics they could be made to the north or the south by simply switching the direction of feed. Very few observations were made to the south, however, so, except as specifically noted, only observations to the north will be discussed in this study. Neither impedance nor antenna pattern measurements were made on the rhombics because of the difficulties involved in getting meaningful results.

A vertical, three-wire Delta antenna was available for use as a receiving antenna. Its height was 70 feet and its base 130 feet. The antenna was fed with 300 ohm Twinlead transmission line and terminated with a 600 ohm resistance.

The receiving rhombic and the Delta antennas were paralleled at the receiver input for most of the oblique sounding records obtained. This was done to enhance the vertical incidence traces on the records. The layer critical frequencies and heights were sometimes necessary in the analysis, and this method provided an easy means of obtaining that data. Tests to determine whether the signal-to-noise ratio was degraded by paralleling the antennas indicated that there was no noticeable decrease. In late 1959 a switching system was installed so that either the Delta or the rhombic could be disconnected from the receiver. The program timer in the recorder was used to automatically control the switching.

B. Typical Sweep Frequency Records.

Groundscatter echoes were the most prevalent type of echo observed in the mid-latitudes, but this was not true in the high latitudes

(e.g. Owren and Stark 1957). Groundscatter was occasionally observed on the sweep frequency sounder, but mostly when the antennas were beamed south. Figure 5 contains four of the best examples of 2F groundscatter recorded with the sweep frequency sounder. Figure 5B is reproduced in Figure 6C for easy reference, and a line drawing of it is contained in Figure 7C. Although the second order vertical incidence trace is weak in Figure 6C, there is little doubt that the 2F echo connects with it. Figure 5D best illustrates this point. Figure 5A is somewhat unusual in that apparently two groundscatter echoes occurred - 2F1 and 2F2. The latter is the echo with the least slope, extending between 7 and 14 Mc/s and 1100 and 2400 km, respectively.

The most frequently observed echo type from the north is illustrated by Figure 8. Figure 8D is reproduced as Figure 6B and is shown as a line drawing in Figure 7B. The significant details of this type of echo are that its range increases linearly with frequency, and it branches off the fundamental vertical incidence trace. The echo was usually observed at night, although it was occasionally observed also during the day. This echo does not show a marked connection with magnetic activity as it occurred nearly every night. It appears to correlate well with spread F, in that if this echo appeared, the vertical incidence F region traces were usually spread as in Figure 8.

Figure 9 shows three records of 2F groundscatter echoes occurring along with echoes that appear to branch off the vertical incidence trace. The significant feature of these latter echoes is that each has approximately one-half the slope and range as the corresponding 2F echo. We term this the 1F echo because of its close relationship with the 2F echo discussed in Chapter 2. Figure 9B is reproduced as Figure 6A and is

shown as a line drawing in Figure 7A. Figure 9D apparently does not contain a 2F echo, but it was included because of its rather odd character. The upper echo has not yet been positively identified.

Figure 10 contains another type of echo which was observed very frequently from the north. In Figure 10D the echo of interest extends from 11 to 24 Mc/s at a range of approximately 1300 km. The fundamental vertical incidence trace extends to approximately 9 Mc/s, and the echo from 9 to 16 Mc/s at 400 to 600 km is probably a 1F echo. We term the echo at 1300 km a 'constant range' echo because of its behavior with frequency. The most significant feature of the echo is the upward hook at the high frequency end; this fact is used in Chapter 5 to show that the echo is produced by direct backscatter from the field aligned boundary of a discrete cloud of F region irregularities.

Figure 11 contains a group of odd echoes which occurred only rarely. In Figure 11D the trace of interest extends from 5 to 11 Mc/s at ranges from 1600 to 3400 km. The echo appears to be a 3F echo (direct scatter 1F echo propagated via one reflection from the F layer each way), except that it is stronger than the 1F echo occurring from 6 to 10 Mc/s at 500 to 900 km. This is difficult to explain without postulating some sort of focusing mechanism depending upon the number of times the energy is incident upon the F layer. These echoes are still unexplained.

Another odd and unidentified group of echoes is illustrated in Figures 12 and 13. Figure 13C is a good example; the interesting echo occurs at 1000 km and appears to be the mirror image, frequency-wise, of the usual vertical incidence traces. We note that both magneto-ionic components exist with approximately the same separation (0.8 Mc/s) as for the vertical incidence traces. The retardation at the low frequency

end of the echo appears to be associated with the F1 layer penetration frequency. The echo apparently was recorded only when the F1 layer was present. If we denote the minimum frequency of the echo as its 'penetration' frequency, assuming that the retardation is caused by its passage through the F1 layer, that penetration frequency unfortunately, does not appear to be related to the F1 critical frequency if a careful analysis is made. The echoes are definitely oblique echoes; this was proven by alternately switching between vertical and oblique antennas. When the antennas were switched in this manner, the echo was always stronger on the oblique antenna during any sequence in which the echo could be identified over a period of at least five consecutive sweeps.

If one assumes that the penetration and the F1 critical frequencies are related by the secant law, the scattering region is determined in space. The observed range of the echo is always too great for direct scatter so a path including reflection from the F2 layer has to be involved. If one tries to assume such a path, the high frequency limit of the echo is usually appreciably above the oblique penetration frequency of the F2 layer. Thus, if one assumes that the secant law holds for the F1 layer, the result, under the above assumptions, is that it does not hold for the F2 layer.

Other seemingly consistent assumptions have always led to a similar contradiction. The only possibility seems to be that there is an appreciable lateral bending of the ray as it penetrates the lower layers, implying large horizontal gradients. If this were true, the echo might then be direct scatter from the F2 region of the same type as the constant range echo, discussed at length in Chapter 5.

Thus far, we have discussed only echoes that primarily involve the F region. A common E region echo is shown in Figure 14. (Figures 14A, 14B, and 14C have 200 km range-marks, while 14D has 100 km marks.) The echo clearly branches off the E region fundamental vertical incidence trace as shown in Figure 14D. It shows the same linear character as the 1F echo, and probably propagates by the same mechanism. In the literature (e.g. Smith 1957) this particular echo is known as the 'slant Es' echo. It correlated well with magnetic activity, in contrast to the 1F and the constant range echoes which apparently did not. In the cases analyzed the magnetic K index lay between 3 and 7 when the slant Es echo occurred. This echo will be discussed further in Chapters 5 and 6.

In general, the 1F echo was a nighttime phenomenon, and the constant range echo was observed during the day. The two were usually observed simultaneously only during the transitional periods of sunrise and sunset. Both echoes increased in strength as winter approached, and decreased in the spring. Their diurnal and seasonal variations will be discussed at length in Chapter 6. The unidentified echoes previously discussed occurred so infrequently that nothing can be said about their diurnal and seasonal variations.

CHAPTER 3.

THE IONOSPHERIC SCATTER PROBLEM

The problem of scatter from ionospheric irregularities is extremely complicated, and, as yet, there is no solution which satisfies everyone. Scatter from irregularities near critical density is especially complex, and although qualitative arguments about its behavior may be intuitively appealing, they may overlook some decisive factor. Until a satisfactory theory is developed, however, qualitative arguments are our only recourse and must be used if we are to attempt to explain even the gross features observed experimentally.

Several recent papers that deal with this subject will be discussed in this chapter. In the first one Herlofson (1952) calculated the energy scattered from a perpendicularly incident wave upon a cylindrical column of electrons in free space. Effects due to collisions and the geomagnetic field were ignored. He considered four separate cases; small and large electron densities, and electric and magnetic polarizations (the polarization type was determined by the electromagnetic field component parallel to the axis of the cylinder). In the case of small densities there was no difference between the two polarizations, and the results agreed with those found by others (e.g. Blackett and Lovell 1941). For large electron densities, however, he found a marked difference; there was a resonance effect in the magnetically polarized scattered field which depended upon the parameters of the cylinder. The echo amplitude was determined by the size of the column and the resonant frequency by the electron density. From this computation Herlofson showed that for a cylinder of electron gas of one density embedded in an electron gas of another density, the resonance effect is possible any time the ratio of the inner to the outer

dielectric constants is minus one (assuming the outer is always positive) and the diameter is proper. He pointed out that it would be theoretically possible for weak irregularities of the proper size near the critical density level to produce a relatively large amount of scatter through the resonance process.

Pitteway (1958) used a perturbation method to calculate the scatter from ionospheric irregularities. His theory was a first order theory so only weak scatter was considered. Collisions were included, but the geomagnetic field was not. He investigated two cases of possible enhancement, first at the oblique reflection level, and second, at the level where the index of refraction was zero. In the first case Pitteway found that at the level of oblique reflection there was at most an enhancement of two or three times that at other levels. Collisions entered decisively into the second case, eliminating, to a great extent, any possible enhancement. Thus, he concluded that there was no appreciable enhancement either by a plasma resonance process such as that proposed by Herlofson or at the level of oblique reflection. He pointed out, however, that his theory was based upon the weak-scatter approximation which is not always valid. He noted that if strong scatter were present, though, most of the energy would be scattered before it reached the proper level, making any possible enhancement from the strong scatter much less significant.

Upon close scrutiny, it is not readily apparent that Pitteway's analysis actually can be compared with Herlofson's. The resonance process proposed by Herlofson applied to strong irregularities while Pitteway carefully noted that his method was valid only for weak irregularities. The resonance process occurred for cylinders when the ratio of the inside

to the outside indices of refraction was -1 by Herlofson's analysis, but Pitteway made his calculation for the level at which the refractive index of the undisturbed medium vanished. Thus, it appears that Pitteway considered the enhancement which was due to the level of vertical incidence reflection, while Herlofson calculated the enhancement that was due to the size and shape of the irregularities. The two computations do not seem to be comparable in spite of Pitteway's claim that they are.

Assuming that they are, however, a further difficulty arises. Pitteway calculated his plasma resonance enhancement at the level where the refractive index was zero. When collisions were introduced, he claimed that the resonance peak disappeared. This disappearance may be due entirely to the fact that he assumed the irregularities were weak and the enhancement occurred at the zero refractive index level. Herlofson's results shows that it is not the absolute value of the refractive index but the ratio of the inside to the outside indices which is important. In the limit of the zero index level, the refractive index inside the irregularity also vanishes. It would seem that the calculation should be made as the zero level is approached rather than at the zero level. Thus, the fact that the singularity is removed when collisions are considered does not appear to disprove the plasma resonance process proposed by Herlofson.

An experimental observation of major importance is that UHF and VHF scatter echoes are obtained only from regions in which the geomagnetic field is essentially normal to the line of sight. Booker (1956a) postulated that this observed aspect sensitivity requires that the wave be almost normally incident upon an elongation parallel to the geomagnetic field. He calculated the scatter from a group of cylindrical irregularities and was able to get fair agreement with existing VHF aspect

sensitivity observations. The theory is not directly applicable to the HF scatter problem, however, because the assumption that the frequency is much larger than the plasma frequency does not hold even approximately in the HF portion of the spectrum. In fact, Owren (1960) pointed out that the theory is useful only in the UHF and VHF regions above 60 Mc/s.

Thus, we have no completely acceptable solution to the HF scatter problem. Herlofson considered cylindrical irregularities but only for the case of normal incidence; thus, no information about allowable aspect angles can be obtained from his theory. Even though Pitteway's theory, in principle, describes weak scatter at oblique incidence, there seems to be no way of obtaining explicit numerical values without resorting to lengthy machine computations. Booker's theory applies only to the case of no refraction, but refraction cannot be ignored in the HF portion of the spectrum. Hence, the scattering process is still largely unexplained although some insight into the problem has been gained.

CHAPTER 4

MODELS FOR THE 1F AND THE CONSTANT RANGE ECHOES

In Chapter 3 we noted that the 1F echo branched off the fundamental F region vertical incidence trace and its range increased linearly with frequency. Figure 15 illustrates this. When the 2F groundscatter trace was present, the range of the 1F echo was approximately one-half that of the corresponding 2F echo. These observations suggest that the echo was caused by scatter at or near the midpoint of the 2F groundscatter path, the point at which the wave was refracted horizontally in the ionosphere (see Figure 2). Thus, the echo must be caused by direct scatter from irregularities at or near the oblique reflection point in the F region.

The production of such irregularities has not been satisfactorily explained. Many early workers believed they could not exist (e.g. Booker 1956b), but during the latter 1950's evidence of the existence of F region irregularities mounted. Peterson et al (1955) obtained auroral type echoes from F region heights. Briggs (1958) used a correlation technique between radio star scintillations and spread F to deduce irregularity heights of 300 km, well into the F region. Parthasarathy et al (1959) obtained heights between 350 and 1000 km using the Russian satellite signals on 20 and 40 Mc/s. Even though we have no explanation for the production of such irregularities, it is increasingly evident that they do exist. This study adds one more bit of evidence on this point.

The shape and the orientation of the irregularities are very critical points. They determine, to a large extent, the direction most favorable for the observation of scatter echoes. Spheres, for example, would have no preferred direction for direct backscatter, but prolate spheroids would. In general, the major portion of the scattered energy is contained on a

conical surface of revolution about the major axis of the irregularity (Booker 1956a). The width of the scattered beam is a function of the elongation of the irregularity - the longer the irregularity, the smaller the beamwidth for a given frequency. For direct backscatter, therefore, the wave must be incident such that the complement of the angle between the wave normal and the major axis of the irregularity differs from zero by no more than the scattering beamwidth angle.

The maximum allowable off-perpendicular angle is the maximum of the complement of the angle between the wave normal and the irregularity major axis for which backscatter can be observed. Because refraction is largely absent, this angle is, in principle, measurable with a reasonable degree of accuracy in the VHF and the UHF portions of the spectrum. In the HF portion, however, refraction affects the results appreciably, and the measurement cannot be made with any precision. Here again, qualitative arguments must be used. The HF echoes were usually fairly well defined, and they originated only from certain directions. From these points one is led to conclude that the maximum allowable off-perpendicular angle for HF scatter echoes from the F region is small. Hence, as a first approximation, we shall require strict normal incidence between the wave and the major axis of the irregularity.

The direction of the major axis of the irregularities is considered next. During the 1950's a substantial amount of evidence accumulated which indicated that the irregularities are elongated along the geomagnetic field. Reference will be made to only a few of these reports because, in some areas of investigation, the amount of published material is quite extensive. Radio auroral backscatter echoes in the VHF and the UHF portions of the spectrum have been definitely shown to originate only

from that part of the E region in which the line of sight perpendicularly intersects the geomagnetic field (e.g. Booker et al 1955, Presnell et al 1959). Peterson et al (1955) reported HF echoes which behaved similarly. Direct scatter echoes observed on the College, HF swept azimuth backscatter sounder tended to be centered geomagnetic north (e.g. Owren, Hunsucker, and Stark 1959). The analysis of radio star scintillation data provides an independent means of showing that the irregularities were field aligned (e.g. Briggs 1958). Thus, the evidence appears conclusive that the irregularities which produced the observed direct backscatter echoes from the ionosphere were elongated along the geomagnetic field.

This appears physically reasonable because an electron can, in general, move more easily along a magnetic line of force than across it. Thus, if an irregularity in the electron density could be produced, it would tend to diffuse along the geomagnetic field, producing an elongated irregularity. Particle collisions modify this diffusion to some extent in the ionosphere. In the E region the mean free path is small so motion is much easier across the field than in the F region where the mean free path is at least a thousand times greater. Hence, F region irregularities should be longer and thinner than those in the E region. This leads to the conclusion that the F region scatter echoes should exhibit more aspect sensitivity than E region echoes, lending support to the assumption of strict normal incidence in the proposed models. Because the high latitude F region echoes have been observed only in the HF spectrum where refraction effects cannot be ignored, no direct aspect sensitivity measurements have been made.

In the following models ray theory is used throughout, collisions are neglected, and the earth and ionosphere are considered plane. Consider

a system of randomly distributed irregularities which are elongated along the geomagnetic field. Assume that normal incidence upon the major axis of the irregularities is required for direct backscatter. To the north of College, the magnetic field is at most 13 degrees off-vertical, so to simplify the problem further, we shall assume that the geomagnetic field is actually vertical in the region of interest. To satisfy the assumed aspect sensitivity requirement, a ray must be horizontal if it is to be scattered back over the path of incidence. Thus, direct backscatter is possible only from those rays which are in the process of being refracted back to earth; those that penetrate the layer cannot satisfy the assumed aspect sensitivity requirement. The angle at which penetration occurs for any given frequency is termed the 'critical angle'. Therefore, under the aspect requirement, direct backscatter is possible only for rays below the critical elevation angle.

Energy will be backscattered for all angles below the critical angle because the scatterers were assumed to be randomly distributed. The amplitude of that portion of the echo which propagates along the path of minimum time (the leading edge) will be strongly enhanced by the least-time focusing mechanism discussed in Chapter 2. Thus, if the echo is weak, only the leading edge will be recorded, just as in the case of 2F groundscatter. The range of the leading edge of the trace as a function of frequency will fall upon the line which passes through the origin and is tangential to the cusp of the fundamental vertical incidence trace.

The echo from the model described above satisfies the observed requirements because the theoretical trace is linear, it branches off the first order vertical incidence trace, and its range is precisely one-half that of the corresponding 2F groundscatter trace. Figure 15 is an

experimentally observed 1F trace. Figure 16 is the calculated trace for direct backscatter from the oblique reflection point (1F echo) in a layer with a parabolic electron density with height. The half thickness is 100 km and the base height 300 km for the layer. Because the scatters in this model are randomly distributed and enhancement is required for the observation of the echo, this mode is termed a weak scatter type 1 mode of propagation.

The slant Es echo shown in Figure 17 exhibits the same sort of character as does the 1F echo, in that its leading edge is well defined, it branches off the fundamental vertical incidence trace, and its range varies linearly with frequency. These observations lead one to conclude that the slant Es echo is produced by energy scattered at or near the oblique reflection point in the E region and enhanced by least-time focusing. This requires a thick layer rather than the usually thin Es layer. Figure 18 contains a line drawing of the high resolution, vertical incidence trace from the College vertical incidence ionosonde for the record shown in Figure 17. The observable retardation shows that the layer is indeed thick and is probably a form classified as retardation Es or Esr. (The National Bureau of Standards Circular by Smith cited previously contains an excellent discussion of the various types of Es that is observed.) Thus, the slant Es echo appears to propagate by the same mechanism as that of the 1F echo and probably should be called the 1Es echo for consistency; the term slant Es is well established, however, so it is retained throughout this discussion.

The basic features of the constant range echo that must be explained are the following, as illustrated in Figure 19 (Figure 20 is a line drawing of Figure 19). The trace is relatively sharp and well defined, its

range is essentially constant out to its junction with the 1F echo, and the trace hooks upward sharply above its junction with the 1F echo. These points suggest that the scattering region is discrete and essentially perpendicular to the wave normal at the oblique reflection point. A field-aligned (essentially vertical) sheet of ionization is immediately suggested. Figure 21 shows the calculated trace from a vertical sheet embedded in the F region 1000 km from the observer, as well as the calculated 1F and the first order vertical incidence traces. The geometry is shown in Figure 22; the normal to the sheet is in the plane of the figure. A parabolic layer having a base height of 300 km and a half thickness of 100 km was used for the computation.

The traces shown in Figures 19 and 21 are clearly similar. Thus, we are led to the conclusion that the constant range echo is produced by the field-aligned boundary of a cloud of F region irregularities. Normal incidence upon the boundary is required in this model, hence, the refraction in the ionosphere is necessary, as for the 1F echo. The soundings illustrated were made to the north so the boundary of the patch must extend east and west.

These conclusions are supported by the observations of Briggs (1958). His analysis of a large group of spread F and radio star scintillation data from mid-latitude stations showed that clouds of field-aligned irregularities exist with boundaries along the lines of constant geomagnetic latitude. All that is required for the production of the constant range echo is that the boundary of such clouds be sharp enough to backscatter energy from an HF wave. As this mode is not enhanced by a focusing agent, it is termed a strong scatter type 1 mode.

CHAPTER 5.

APPLICATIONS OF THESE ECHOES TO IONOSPHERIC RESEARCH

With the aid of the F region direct scatter echoes we can examine the spatial and the temporal behavior of the F layer irregularities. Using the method outlined below, one can obtain directly the height of the irregularities producing a given 1F echo, provided the vertical incidence trace is reasonably clear. The echoes shown in Figure 23, however, would be difficult to scale because of the uncertainty in determining the critical frequency.

The vertical incidence limit of the oblique path of minimum time occurs at the branch frequency f_t (see Chapter 2). Thus, the true height of the irregularities equals that of the vertical incidence reflection at the frequency f_t . The determination of the height of the irregularities in the F region requires just the computation of the true height of reflection for the frequency f_t . The easiest way of doing this is to use the graphical method of Schmerling (1957) which was devised from Budden's (1955) more complicated method requiring a digital computer. The National Bureau of Standards has developed overlays which greatly simplify the application of Schmerling's method (Wright and Norton 1959). Using the materials supplied by NBS, one can obtain a complete electron density - true height profile in a few minutes. To determine the irregularity height from the 1F echo, though, one need only compute the true height of reflection for f_t , a single calculation that is completed very quickly.

The general range of heights for the irregularities producing the 1F echo can be obtained from the following discussion. The base of the usual arctic F layer lies between 200 and 300 km. A half-thickness of 100 km is reasonable so the height of the layer maximum lies in the range between

300 and 400 km. The path of least time is reflected from a level between five- and six-tenths of the distance between the base and the maximum of the F layer (assuming a parabolic electron distribution). Thus, the irregularities which produce the LF echo lie, in general, at heights between 250 and 350 km.

The production of the LF echo requires that the irregularities exist at a particular height in the ionosphere. Because the LF echo is observed so regularly, it is highly improbable that the irregularities are confined only to that particular level. Hence, the irregularities extend vertically throughout much of the F region below, and probably above, the layer maximum. This conclusion is supported by Parthasarathy et al (1959) who found clouds between 350 and 1000 km in the ionosphere.

At night the LF trace is usually continuous, but its slope varies with frequency in a manner which suggests that instead of a purely random distribution of irregularities, we are dealing with large clouds of random irregularities. In the following discussion we shall find the meteorological terms for cloud distribution (scattered, broken, and overcast, in that order for increasing cloudiness) quite useful. Figure 23A illustrates a LF echo which exhibits considerable structure. The ordinary and the extraordinary critical frequencies appear to be between 2.9 and 3.0 Mc/s, and 3.6 and 3.7 Mc/s, respectively. The oblique echo probably starts near 3.2 or 3.3 Mc/s¹. Between the start and the end of the oblique echo, one can identify three parts which appear to be three constant range echoes as shown in the accompanying line drawing, Figure 24. The constant range

¹If one examines the College high resolution vertical incidence sounder records, the start of the LF echo can usually be identified when the echo is strong on the oblique sounder. When this echo is observed on the vertical incidence equipment (it is usually called the 'polar spur'), it appears to branch off the extraordinary trace.

echo is produced by scatter from the boundary of a cloud of irregularities so three distinct clouds probably produced the trace shown. This effect might be explained by assuming horizontal electron density gradients, but it is difficult to see how the particular record could be produced by such gradients. Thus, the cloud theory appears to be the likely one.

The size of the clouds can also be estimated from the structure of the echoes. A cloud that is comparable to the pulse width would produce just a constant range echo, while a large cloud of irregularities to the north of the observer would produce first (in frequency), a constant range echo, and then a sloping 1F echo when the least time rays penetrate into the cloud. As long as the frequency is low enough that the wave is perpendicularly incident upon the boundary of the cloud, the constant range echo is observed. For high frequencies, though, the ionospheric refraction is no longer sufficient to produce perpendicularity at the boundary; the wave penetrates into the cloud and is scattered from the irregularities within it, producing the weak scatter 1F echo.

The echo shown in Figure 23B appears to be produced by several moderately large, closely spaced clouds. In meteorological terms this type of cloud cover would be called broken. The trace in Figure 23C is continuous and shows very little structure except at the high frequency end, indicating that the cloud cover was in the form of an overcast. Figure 27D is a good example of small, distinct (scattered) clouds because the echoes are narrow and show little slope at the high frequency end.

From the temporal variation of the echoes we deduce that solar radiation tends to 'smooth' the ionosphere. The cloud size and distribution appear to depend mostly upon local time. Thus, during the day only

scattered clouds were observed. During the transitional periods near sunrise and sunset the cloud cover was broken, and the nights broken to overcast, depending upon the season. Generally, the cloud cover was denser at a given time of day in the winter than in the summer.

There does not appear to be any correlation between magnetic disturbances and the F region cloud cover. This may be primarily the result of the increased absorption that generally occurred along with the magnetic disturbance; the lack of a sufficient amount of data for a reliable statistical study may also contribute to this¹. The absorption tended to reduce the amplitude of the scatter echoes, which, in turn, probably reduced the number of echoes observed. During severe disturbances very few, if any, F region scatter echoes were observed. Until a careful statistical analysis can be made on better data than are available, the question of the connection with magnetic disturbances must remain open. Because the scatter echoes were observed during quiet as well as moderately disturbed periods, however, we must tentatively conclude that the variation in the density of the irregularities was primarily diurnal and did not depend markedly upon the magnetic conditions.

The 1F echo was generally a nighttime phenomenon. It appeared near sunset and disappeared near sunrise. Its strength varied mostly with local time, being strongest in the early morning hours. The overcast condition usually occurred near midnight and persisted until dawn. During

¹A statistical analysis of the data would be difficult to justify because of the unreliability of the equipment. Fully fifty per cent of the possible observations were lost because various randomly occurring circuit failures (e.g. camera jams or circuit breakers opening unnecessarily) shut down the equipment. Other failures (e.g. tube failures, improper adjustment, or instability in various circuits) allowed the equipment to run but degraded the overall system sensitivity. The majority of the echoes were of marginal strength, at best, so a small decrease in system sensitivity substantially reduced the number of observed echoes. Thus, the absence of echoes during any particular period might be entirely equipmental.

the summer months when the ionosphere was illuminated all the time, the 1F echo was usually weak and occurred only near midnight. In the winter when the nights were long, it was usually stronger and lasted for many hours. Unfortunately, the available summer data are not as reliable as the winter data so the yearly variation is still somewhat open to question. Generally, though, the more darkness, the stronger the echoes were. The 1F echo usually occurred only when the vertical incidence trace was spread. Its strength appeared to vary with the amount of spread, although here again the data are unreliable.

The constant range echo was observed only during those daylight periods when solar radiation passed obliquely through the ionosphere. During the midday period in the summer the constant range echo was not observed. Twelve days each from August and September 1959 were examined and there were no identifiable F region direct scatter echoes recorded during midday, even though part of the period was very disturbed magnetically. When the vertical incidence traces were clearly defined, no oblique echoes of any sort were observed. The constant range and the 1F echo appeared only when the vertical incidence trace was spread. Thus, there appears to be a connection between F region cloudiness and spread F.

To further investigate the temporal variations of the 1F and the constant range echoes, three sequences of records are shown and discussed in detail. Figures 25 and 26 contain records selected from the mornings of 16 November and 20 December 1958, and Figure 27 the afternoon of 20 December 1958.

The first five records shown in Figure 25 were taken fifteen minutes apart, starting at 0715, and show the speed of the events. In Figure 25A, recorded at 0715 (all times are local or 150° WMT), the vertical incidence

traces are so spread that the F region critical frequency cannot be determined. The 1F echo appears to branch off the vertical incidence trace in the vicinity of 8 Mc/s; it disappears near 12 Mc/s, reappears at 15 Mc/s, and finally disappears at 21 Mc/s. A constant range echo at 1000 km extends between 10 and 15 Mc/s. The echoes appearing at 1800 and 2400 km between 5 and 12 Mc/s are unidentified; in the rest of the discussion these echoes will be ignored.

In the next four records, Figures 25B through 25E the constant range echo at 1000 km stays more or less fixed in range. The 1F echo gradually disappears, and a second constant range trace appears at 1200 km. The critical frequency probably remains about the same, but the vertical incidence trace is noticeably less spread by 0820, Figure 25E.

Figure 25F was taken at 1106 and shows a normal winter day record. The vertical incidence traces are well defined, and a weak 2F groundscatter echo extends between 800 and 1000 km between 11 and 13 Mc/s, respectively. The constant range echo appears at 1200 km, and no 1F is present.

Figure 26A, taken at 0635, shows a well defined 1F echo extending from approximately 7 to 17 Mc/s and a constant range echo from 8 to 17 Mc/s. The 1F trace starts at 500 km and ends at its junction with the constant range echo at 1400 km. The vertical incidence fundamental trace is spread and poorly defined. A weak, second order Es echo is present just above the 200 km range-mark, and the second order vertical incidence trace from the F layer is shown weakly.

In Figure 26B, recorded at 0720, we note that the 1F echo no longer connects with the vertical incidence trace, indicating that the irregularities overhead have disappeared. The vertical incidence trace is clearer than earlier in the day. The constant range echo is considerably weaker and extends from 10 to 16 Mc/s at a range of 1400 km.

By 0805, Figure 26C, the vertical incidence trace is definitely clearer and the critical frequency has increased. The 1F echo does not appear between 8 and 13 Mc/s; in fact, it appears only at ranges greater than the 1000 km range of the constant range echo. The latter echo is weak and diffuse, indicating that the boundary of the scattering cloud is not sharply defined. The constant range trace may be composed of two distinct echoes, one at 1000 km and the second at 1200.

At 0905, Figure 26D, the constant range echo has moved into 900 km and has become sharp and well defined. Again we note that the 1F echo exists only at ranges greater than that of the constant range echo. The vertical incidence trace is much clearer, and the critical frequency has increased to approximately 9 Mc/s.

By 0950, Figure 26E, the constant range echo has moved out to 1100 km and is considerably spread. The extraordinary critical frequency is about 11 Mc/s, and the 1F echo appears only beyond the constant range echo. Ground sunrise at College was at 0958.

Figure 26F shows a strong constant range echo at 1100 km that extends from 10 to 23 Mc/s. A weak 2F groundscatter echo branches off the second order vertical incidence trace and extends between 12 and 15 Mc/s at ranges from 800 to 1100 km, respectively. This appears to be a typical winter day record.

Figure 27A, taken at 1435, is again a reasonably normal daytime record. The vertical incidence traces are clear, and there are constant range traces at 1200 and 1500 km. Between 13 and 15 Mc/s, and 800 and 1000 km, respectively, 2F groundscatter is present but very weak. The extraordinary critical frequency is approximately 13.8 Mc/s. Ground sunset occurred at 1336.

At 1550, Figure 27B, the nearest constant range echo has decreased in range to 1100 km, and it now shows the characteristic high frequency cut-off at its junction with the 1F echo. Again the vertical incidence traces are clear, and the 2F echo is still present. The critical frequency has decreased by about half a megacycle per second.

The records in Figures 27B through 27F were taken fifteen minutes apart, indicating the speed of occurrence of the events. In Figure 27C the strongest constant range echo is at 1000 km, but a weak echo has also appeared at 800 km. The critical frequency has decreased by several hundred kilocycles per second, and the vertical incidence traces are still clear.

Figures 27D, 27E, and 27F show the continuation of this sequence of events. The range of the constant range echoes decreases, the critical frequency decreases, and the 1F echo appears at a progressively shorter range, but always at a longer range than the constant range echo.

Figure 27G was taken at 1750, an hour after Figure 27F. By this time the 1F echo was well established and had merged with the vertical incidence trace. The vertical incidence trace was spreading, and the extraordinary critical frequency was approximately 9 Mc/s.

In general, the records indicate that F region cloudiness depended upon the absence of solar radiation. In the summer when the altitude of the sun was high during the day, there was little or no F region cloudiness. During mornings and evenings when the solar radiation struck the atmosphere obliquely, the cloud cover was mostly broken, the density increasing with darkness. In the winter the sun was always low on the horizon, and the F region was partly cloudy most of the day. During the

winter sunrise and sunset periods the F region was quite cloudy, and at night it was mostly overcast.

The extent of the F region cloudiness apparently was not dependent upon the critical frequency. In the winter the F region critical frequency was high during the day, 10 to 15 Mc/s, decreasing to 2 to 4 Mc/s at night; in the summer the variation was much smaller, 5 to 8 Mc/s during the day, and 2 to 4 Mc/s at night. The controlling factor appears to be the zenith angle of the sun's radiation, although the extent of the cloudiness may be connected somehow with the rate of electron production or disappearance as well as the prevailing magnetic conditions.

In the discussion above we were concerned only with the F region echoes. Even though the same echo modes are observed from the E region as from the F region, there did not appear to be any connection between the production of the E and the F region echoes. The E region echoes appeared only during moderate to severe magnetic disturbances. Furthermore, the slant Es echo was observed during all periods of the day, while the 1F echo was rarely recorded during daylight hours.

When the slant Es echo appeared, the usual sequence of events was as follows. The F region echoes disappeared or became very weak, then the slant Es echo would appear. It would branch off the first order, vertical incidence, E region trace and extend upward in range to 400 or 500 km at 15 to 20 Mc/s. The high frequency end of the slant Es echo would first increase in frequency to or above 25 Mc/s and then decrease. During this period the low frequency end of the echo would separate from the vertical incidence trace, forming into a constant range echo at the low frequencies and a slanting echo at the high frequencies. This first phase averaged one to two hours in length. As time progressed further,

the echo would break up into one or more constant range echoes, lasting sometimes for many hours. Occasionally the constant range phase was completely missing; in this case the records generally indicated a complete blackout.

The slant Es echo occurred only during disturbed periods. This observation led to the question of whether it was an auroral type echo which was detected also at VHF. The echo was usually strong between 20 and 25 Mc/s on the College oblique, sweep frequency sounder even though the system sensitivity dropped rapidly above 23 Mc/s, so a comparison study was made between the sweep frequency sounder and the simultaneous 41 Mc/s College radar observations (Leonard 1959). Fourteen sequences of slant Es were chosen from the sweep frequency records of November and December 1958 for comparison. There were coincident films from the 41 Mc/s radar on 10 occasions. Table 6.1 contains some of the pertinent information on these records. The times listed are the times during which an identifiable slant Es echo was recorded by the sweep frequency sounder. Approximate E region sunrise at College is shown; sunrise 5 degrees to the north was approximately one hour later, indicating that the observations listed in Table 6.1 were made when the E region was generally dark. Sunlight does not appear to be a controlling factor, however, because the slant Es echo has been observed during all periods of the day. The K indices were derived from a rough average of the magnetic activity at College during the periods listed.

A careful analysis showed that in 9 out of these 10 cases, when the slant Es echo on the sweep frequency sounder extended beyond 23 Mc/s, an echo was also observed on the 41 Mc/s radar at the same range as that reached by the high frequency end of the slant Es echo. In the exceptional

Table 1.

Date	Time		Number of C4 Records	E Region Sunrise	K
	150° Start	WMT End			
20 November 1958	0000	0500	21	0640	3
25 " "	0245	0745	21	0655	5
27 " "	0415	0730	14	0700	4
29 " "	0200	0400	9	0705	5
13 December "	0345	0600	10	0730	7
14 " "	0415	0815	17	0735	6
17 " "	0645	0830	8	0740	7
26-27 " "	2315	0400	20	0740	5
28 " "	0445	0600	5	0735	5
5 January 1959	0645	0815	7	0720	6

case the high frequency limit of the echo varied between 22 and 25 Mc/s over a period of several hours, and while an echo existed on the 41 Mc/s radar at the proper range during part of the time, there was a period of an hour when the sweep frequency echo extended to 24 or 25 Mc/s but no 41 Mc/s echo appeared.

Generally, however, the agreement was good. The 41 Mc/s radar echo would usually appear or disappear depending on whether or not the slant Es echo extended above 23 Mc/s. Figures 28 and 29 show one of the best examples of this. Figure 28 contains a selected group of sweep frequency records from the morning of 28 December 1958; Figure 29 illustrates the continuous record for the College 41 Mc/s IGY Auroral Radar for the period 0400 to 0630 150° WMT, 28 December 1958.

Between 0300 and 0400 both the sweep frequency and the 41 Mc/s records show no oblique echoes of any kind. Figure 28A is typical of that period for the sweep frequency sounder. At 0436, Figure 28B, a weak, sloping echo appears between 10 and 23 Mc/s on the sweep frequency sounder, but no corresponding echo appears on the 41 Mc/s radar. By 0451, Figure 28C, the slant Es echo is fairly well established, and an echo at 500 km has appeared on the 41 Mc/s radar in Figure 29. Just above 23 Mc/s the range of the slant Es echo is approximately 500 km; thus, the echoes seem to agree. The next two sweep frequency records are essentially the same as Figure 28C. Even though the 41 Mc/s radar echo fades in and out, it is present during all of the sweep frequency observations between 0445 and 0606. (The interference caused by the sweep frequency sounder when it operated is clearly visible on the original 41 Mc/s radar film.)

Figures 28D, 28E, and 28F, recorded at 0536, 0551, and 0606, respectively, show the typical progression of events; at 0536 the low frequency

end of the echo no longer slopes downward, indicating that the southern boundary of the scattering irregularities is to the north of College. The minimum range is 400 km so the cloud is approximately 400 km away. The 0551 record shows no slope to the slant Es echo except possibly at the high frequency end, and the minimum range is approximately 600 km. The 0606 sweep shows the same type of echo except that it has become weaker. After the 0606 sweep both the sweep frequency and the 41 Mc/s radar echoes disappear.

Typically, the slant Es echo was composed of three main parts. The range was constant over the low frequency end of the trace, then sloped upward towards 600 km as the frequency increased, and finally became essentially constant again above 600 km. This structure can be qualitatively explained by the following model.

Assume that a large cloud of field-aligned irregularities exists somewhere to the north of an observer in the northern hemisphere and that the boundary of the cloud is both field-aligned and sharp enough to back-scatter energy from any wave that is normally-incident upon it. Then, up to the frequency at which the least-time path is perpendicularly incident upon the boundary, the echo will be essentially constant in range, corresponding to the strong scatter F region echo discussed in Chapter 5. Above that frequency the weak scatter from the interior of the cloud will predominate, producing that part of the echo which slants upward. This explains the first two features noted above. The third feature, the constant range part at the high frequency end of the sweep, can be explained from geometrical and aspect sensitivity consideration.

For E region heights to the north of College, the line of sight approaches normal incidence to the magnetic field most closely at

approximately 700 km (Leadabrand et al 1959). Hence, as the frequency increases and the range of the weak-scatter echo approaches 600 km, the line of sight becomes more and more nearly perpendicular to the geomagnetic field, and one would expect that the slope of the leading edge of the echo would decrease as the frequency continues to increase. There are two focusing effects operating here - least-time and aspect-sensitivity focusing. The first produces a sloping echo, and the second a constant range echo. Thus, one would expect the combination of these focusing effects to produce a flattening of the trace at the high frequency end.

The E region echoes occurred much less frequently than those from the F region. Because of the broad pulse that was necessary, very little structure would be detectable in the E region echoes even if it were there. Thus, it is difficult to obtain information on the extent of the E region clouds. The trace shown in Figure 17 was obtained using a 200 microsecond pulse (one-third that used for the rest of the illustrated records) and shows almost no variation in trace width with frequency. From that record one would infer a cloud of randomly distributed irregularities of at least 600 km in north-south extent. Visual auroras seldom extend over such a great range in latitude, so explaining the cause of the slant Es echo is difficult by assuming that the scatterers are, in some manner, connected with visual auroras. Thus, while we know that both the slant Es echo and visual auroras are related to magnetic activity, we still can not explain the origin of the scatterers which produce the slant Es echo.

CHAPTER 6.

RECOMMENDATIONS FOR FURTHER RESEARCH

The investigation reported here has raised many questions which remain unanswered. Their explanations would be an important contribution to the knowledge of the ionosphere. Some of the problems are listed below.

1. The F region echoes generally disappeared during disturbances. This cannot be wholly due to D region absorption because E region echoes were strong during periods when the F region echoes were completely gone. Much higher system sensitivity is needed to investigate this problem.
2. An appreciable amount of energy is scattered by the F region irregularities as evidenced by the strength of the echoes. Whether or not the amplitude of the incident wave is appreciably diminished is an interesting problem. A significant decrease in the incident wave would provide a simple solution to the problem of why groundscatter is only rarely observed from the north.
3. Echoes from the F region should be more aspect sensitive than those from the E region by theoretical considerations. A high-powered, very narrow pulse would be necessary to determine the aspect sensitivity requirement for the F region echoes. This might also solve the problem of why the 1F and the constant range echoes were apparently not observed from the south.
4. One of the major problems, of course, is the cause of the F region irregularities. Magnetic activity should affect the F region as it affects the E region, but this does not seem to be so. The increase in the ionospheric absorption during a disturbance may be a significant factor because any possible F region echoes might be completely absorbed. Solar

control of the F region irregularities is definite, but the detailed diurnal and seasonal variations are still unknown.

5. The determination of the contribution of each of the magneto-ionic components to the scatter echoes might well lead to an understanding of the ionospheric scattering mechanism. The LF echo is apparently caused by the extraordinary component. This seems reasonable to some extent because the magnetic field affects the extraordinary component to a much greater degree than the ordinary component.

An increase of at least twenty decibels in the overall system sensitivity could produce answers to many of these questions. Some of the echoes that were recorded only occasionally on the present equipment would probably become regularly observable and could be identified. Such an increase in sensitivity is technically possible.

The present equipment is not adequate for statistical investigations of the F region irregularities or for determining the propagation modes of the many unexplained echoes such as those discussed in Chapter 3. Two reasons are that the system sensitivity was neither high enough nor constant enough over an extended period of time. To remedy these difficulties either major rebuilding or new equipment is necessary.

CHAPTER 7.

CONCLUSIONS

The 1F and the constant range echoes represent two regularly observed types of HF backscatter at College, Alaska. The 1F trace branches off the fundamental vertical incidence trace and increases approximately linearly in range with frequency. The range of the constant range echo is nearly constant below the frequency at which it joins the 1F echo; above the junction the range increases sharply. The 1F and the constant range echoes generally occurred together only during the sunrise and sunset periods. The constant range echo predominated in the daytime and the 1F at night. Both were observed more frequently in the winter than in the summer.

These echoes were direct backscatter from irregularities in the F region electron density. The echoes were produced by energy scattered near the oblique reflection point where the ray is approximately horizontal in the ionosphere; this aspect sensitivity indicates that the irregularities are elongated with major axes essentially vertical. On the College swept azimuth backscatter sounder these echoes were generally centered about geomagnetic north. Thus, we are led to conclude that the irregularities were aligned along the geomagnetic field rather than strictly vertical.

The 1F echo was produced by least-time focused backscatter from a random distribution of F region irregularities. A close examination of the 1F echo indicated that the irregularities were usually distributed within regions limited in north-south extent. We term such regions embedded in the F layer 'clouds'.

The constant range echo is produced by scatter from the boundary of one of these clouds of irregularities. No enhancement is required for the observation of this echo so it is termed a strong scatter echo, in contrast to the weak scatter 1F echo.

The true height of the irregularities can be directly determined from the 1F echo. Heights in the range from 250 to 350 km were found by this technique. The 1F echo was produced only at a particular height for a given F region; thus, because of the great regularity with which the 1F echo appeared, it seems reasonable to conclude that the irregularities extended up to and probably considerably beyond the F region maximum.

A detailed examination of the records indicated that the density and size of the clouds varied with solar radiation. During the day the clouds were small and widely scattered. Near the transitional periods of sunrise and sunset the clouds were more numerous and larger. During the summer night the clouds were large and numerous and during the winter night the clouds usually completely covered the F region. Thus, the effect of solar radiation was to 'smooth' the ionosphere.

The 1F echo does not appear to be associated with magnetic activity because it occurred nearly every night. This point is uncertain, though, because the lack of reliability of the equipment made a statistical study impossible. It is evident, however, that solar radiation played a more important role than did magnetic activity in the production of the scattering irregularities in the F region.

Magnetic activity had a profound effect on the E region echoes. The slant Es echo was observed only when the magnetic K index was between 3 and 7. Hence, it would appear that magnetic activity should also

affect the F region. Further study is needed on this point; it might produce the explanation of the cause of the F region irregularities.

Further work with greatly increased system sensitivity is indicated by this study. Such a program should produce a significant advance in the knowledge of the auroral zone ionosphere.

ACKNOWLEDGEMENTS

The author wishes to thank Dr. Leif Owren for his helpful assistance, discussions, and criticism. Drs. Gian-Carlo Rumi and George Reid proposed several fruitful ideas during the early part of the work. Mr. Robert Leonard helped scale the auroral radar film, and his subsequent discussions of the results were most helpful.

The research reported in this document has been sponsored by the Electronic Research Directorate of the Air Force Cambridge Research Laboratories, Air Force Research Division, under Contracts No. AF 19(604)-1859 and AF 19(604)-5574.

BIBLIOGRAPHY

- Abel, W. G., and L. C. Edwards, The source of long distance backscatter, Proc. Inst. Radio Engrs., 39, 1538-1541, Dec. 1951.
- Appleton, E. V., and W. J. G. Beynon, The application of ionospheric data to radio communication, Part I, Proc. Phys. Soc. 52, 518-533, 1940.
- Benner, A. H., Predicting maximum usable frequency from long distance scatter, Proc. Inst. Radio Engrs., 37, 44-47, Jan. 1949.
- Blackett, P. M. S., and A. C. B. Lovell, Radio echoes and cosmic ray showers, Proc. Roy. Soc. A, 177, 183-186, 1941.
- Booker, H. G., C. W. Gartlein, and B. Nichols, Interpretations of radio reflections from the aurora, J. Geophys. Research, 60, 1-22, Mar. 1955.
- Booker, H. G., A theory of scattering by non-isotropic irregularities with application to radar reflections from aurora, J. Atmospheric and Terrest. Phys., 8, 204-221, May 1956. (a)
- Booker, H. G., Turbulence in the ionosphere with applications to meteor trails, radio star scintillations, auroral radar echoes, and other phenomena, J. Geophys. Research, 61, 12, 673-705, Dec. 1956. (b)
- Briggs, B. H., A study of the ionospheric irregularities which cause spread-F echoes and scintillations of radio stars, J. Atmospheric and Terrest. Phys., 12, 1, 34-45, 1958.
- Brown, J. N., Automatic sweep-frequency ionospheric recorder, Model C4, Proc. Inst. Radio Engrs., 74, 296-300, Feb. 1959.
- Budden, K. G., A method for determining the variation of electron density with height ($N(z)$ curves) from curves of equivalent height against frequency ($h' f$ curves), Report of the Physical Society Conference on the Physics of the Ionosphere, Cavendish Laboratory, Cambridge, 1955.
- Chapman, J. H., K. Davies, and C. A. Littlewood, Radio observations of the ionosphere at oblique incidence, Can. J. Phys., 33, 713-722, Dec. 1955.
- Dieminger, W., The scattering of radio waves, Proc. Phys. Soc. B64, 142-158, Feb. 1951.
- Eckersley, T. L., Studies in radio transmission, J. Inst. Elec. Engrs., 71, 434-443, 1932.
- Eckersley, T. L., Irregular ionic clouds in the E layer of the ionosphere, Nature, 140, 846, 1937.

- Eckersley, T. L., Scattering of wireless waves in the ionosphere, *Nature*, 143, 33-34, Jan. 7, 1939.
- Eckersley, T. L., Analysis of the effect of scattering in radio transmission, *J. Inst. Elec. Engrs.*, 86, 548-563, June 1940.
- Eckersley, T. L., G. Millington, and J. W. Cox, Ground and cloud scatter of electromagnetic radiation, *Nature*, 153, 341, March 18, 1944.
- Eckersley, T. L., Observations of scatter clouds, *Nature*, 162, 24-25, July 3, 1948.
- Edwards, C. F., and K. G. Jansky, Measurements of the delay and direction of arrival of echoes from nearby short wave transmitters, *Proc. Inst. Radio Engrs.*, 29, 322-329, June 1941.
- Gates, H. P., Observations of long distance pulse propagation, Interim report, Aug. 1947 to July 1948, U.S. Navy Electronics Laboratory Report 116, April 5, 1949.
- Hartsfield, W. L., S. M. Ostrow, and R. Silberstein, Backscatter observations by the CRPL, Aug. 1947 to Mar. 1948, *J. Research N.B.S.* 44, 199-214, Feb., 1950.
- Herlofson, N., Plasma resonance in ionospheric irregularities, *Ark. Fys.*, 3, 15, 247-297, 1952.
- Hoag, J. B., and V. J. Andrew, A study of short time multiple echoes, *Proc. Inst. Radio Engrs.*, 16, 1368-1374, Oct. 1928.
- Leadabrand, R. L., L. T. Dolphin, Jr., and A. M. Peterson, Preliminary results of 400 Mc radar investigations of auroral echoes at College, Alaska, *Trans. Inst. Radio Engrs.* AP-7, 2, 127-136, April 1959.
- Leonard, R. S., A low power VHF radar for auroral research, *Proc. Inst. Radio Engrs.*, 47, 320-322, Feb. 1959.
- McCue, C. G., High-frequency backscatter at Salisbury, South Australia, *Aust. J. Phys.*, 9, 454-470, Dec. 1956.
- Owren, L., R. D. Hunsucker, and R. A. Stark, Final Report, Contract No. AF 19(604)-1859, Geophysical Institute, University of Alaska, Oct. 1959.
- Owren, L., High latitude radio aurora, Paper presented at Commission 3, XIII General Assembly of U.R.S.I., 1960.
- Parthasarathy, R., R. P. Basler, and R. N. DeWitt, A new method for studying the auroral ionosphere using earth satellites, *Proc. Inst. Radio Engrs.*, 47, 9, 1660, Sept. 1959.
- Peterson, A. M., The interpretation of long scatter echo patterns, *J. Geophys. Research*, 54, 284, Sept. 1949.

- Peterson, A. M., The mechanism of F-layer propagated backscatter echoes, J. Geophys. Research, 56, 221-237, June 1951.
- Peterson, A. M., O. G. Villard, Jr., and R. L. Leadabrand, Regularly observable aspect sensitive radio reflections from ionization aligned with the earth's magnetic field and located within the ionospheric layers at middle latitudes, J. Geophys. Research, 60, 497-512, Dec. 1955.
- Pierce, J. A., and H. R. Mimno, Reception of radio echoes from distant ionospheric irregularities, Phys. Rev., 57, 95-105, Jan. 1940.
- Pitteway, M. L. V., The reflection of radio waves from a stratified ionosphere modified by weak irregularities, Proc. Roy. Soc., A 246, 1247, 556-567, Aug. 26, 1958.
- Presnell, R. I., R. L. Leadabrand, A. M. Peterson, R. B. Dyce, J. C. Schlobohm, and M. R. Berg, VHF and UHF radar observations of the aurora at College, Alaska, J. Geophys. Research, 64, 1179-1190, Sept. 1959.
- Quack, E., and H. Mogel, Short range echoes with short waves, Proc. Inst. Radio Engrs., 17, 824-829, May 1929.
- Schmerling, E. R., An easily applied method for the reduction of h'-f records to N-h profiles including the effects of the earth's magnetic field, J. Atmospheric and Terrest. Phys., 12, 1, 8-16, 1958.
- Silberstein, R., Oblique incidence propagation work of the CRPL, J. Geophys. Research, 54, 288, Sept. 1949.
- Silberstein, R., Sweep frequency backscatter - some observations and deductions, Trans. Inst. Radio Engrs., AP-2, 56-63, 1954.
- Smith, E. K., Worldwide Occurrence of Sporadic E, Circular 582, National Bureau of Standards, March 1957.
- Sulzer, P. G., Sweep frequency pulse transmission measurements over a 2400 km path, J. Geophys. Research, 60, 411-420, Dec. 1955.
- Taylor, A. H., and L. C. Young, Studies of high-frequency radio wave propagation, Proc. Inst. Radio Engrs., 16, 561-578, May 1928.
- Taylor, A. H., and L. C. Young, Studies of echo signals, Proc. Inst. Radio Engrs., 17, 1491-1507, Sept. 1929.
- Wieder, B., Some results of a sweep frequency propagation experiment over an 1150 km EW path, J. Geophys. Research, 60, 395-409, Dec. 1955.
- Wright, J. W., and R. B. Norton, Analysis of ionospheric vertical soundings for electron density profile data, Technical Note 14, Boulder Laboratory, National Bureau of Standards, July 1959.

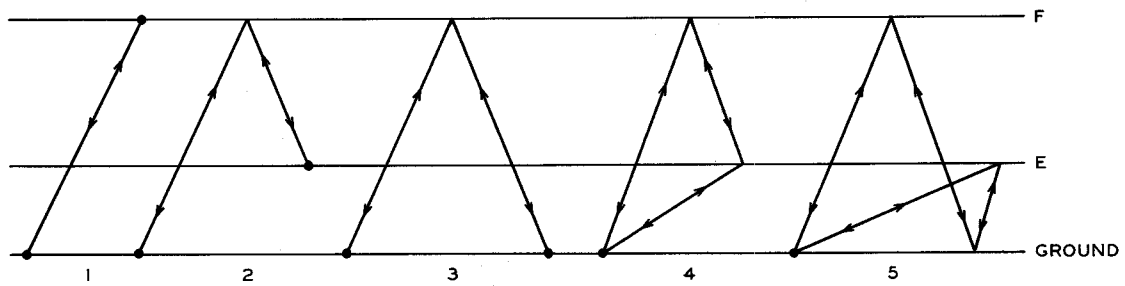


Fig. 1. Possible backscatter mode types.

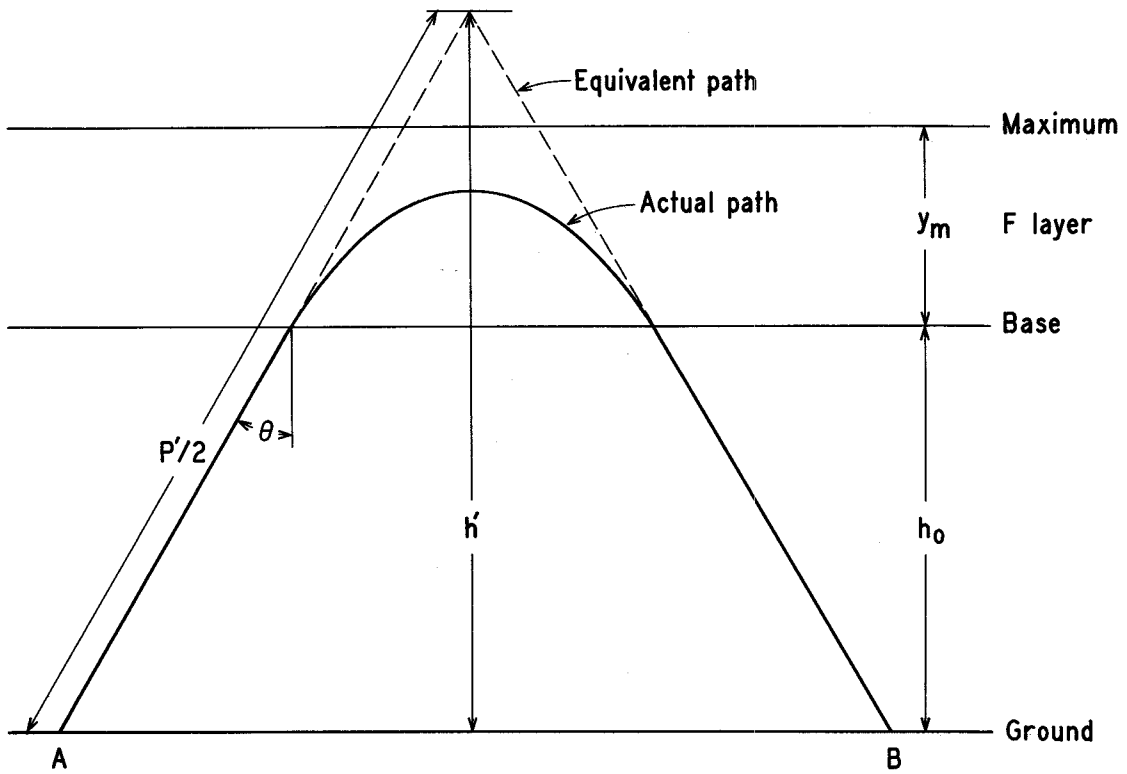


Fig. 2. Equivalent and actual path geometry.

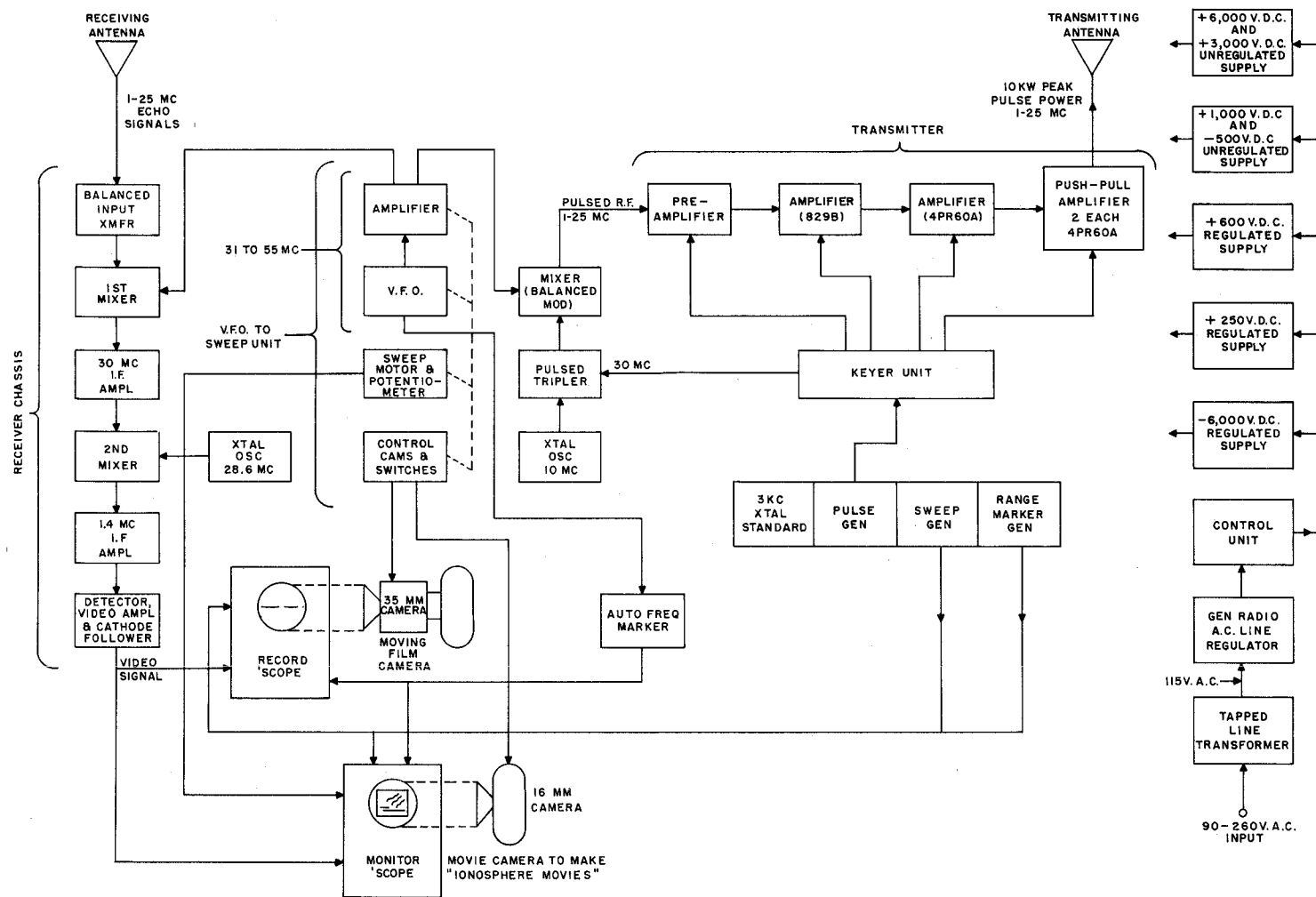


Fig. 3. Block diagram of NBS Model C4 ionosonde.

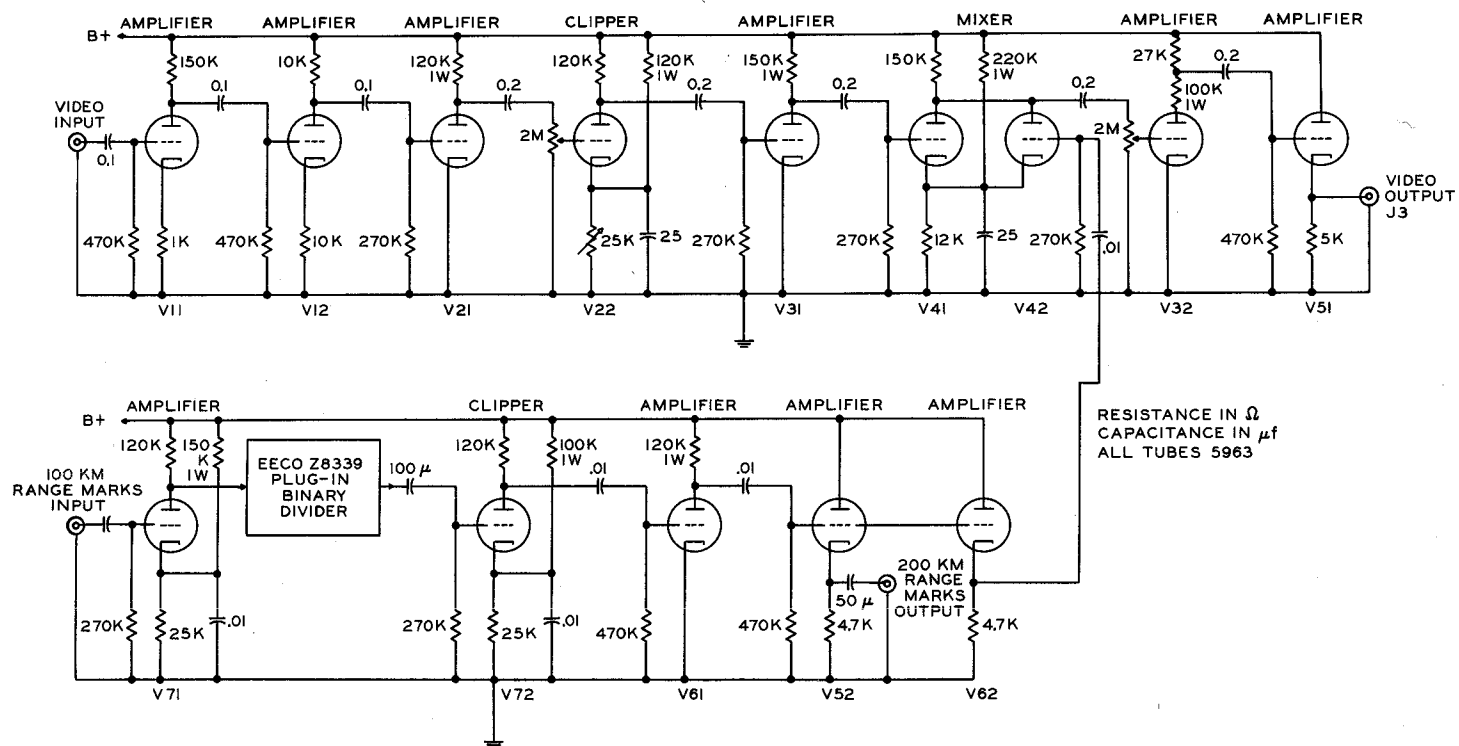


Fig. 4. Clipper-mixer amplifier diagram.

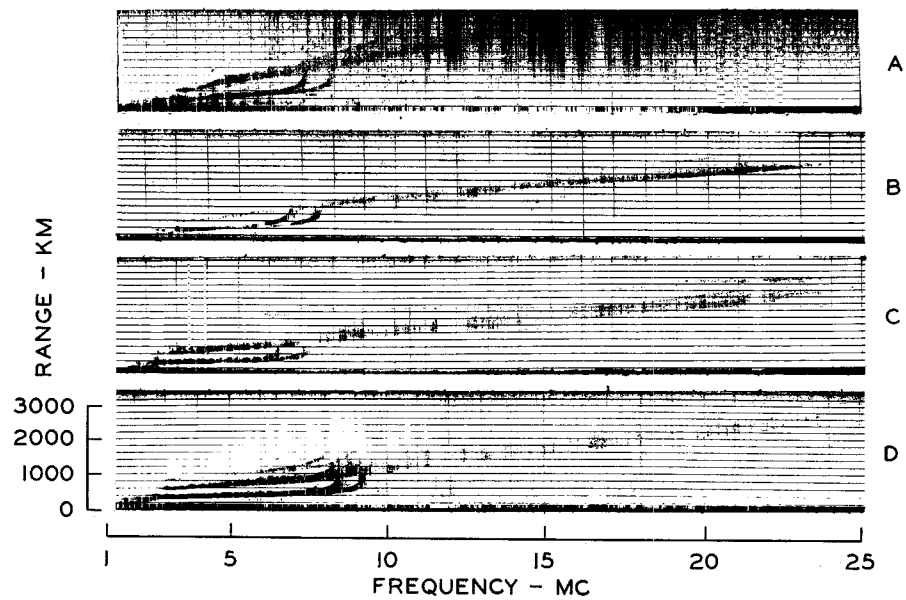


Fig. 5. Examples of 2F groundscatter echoes.

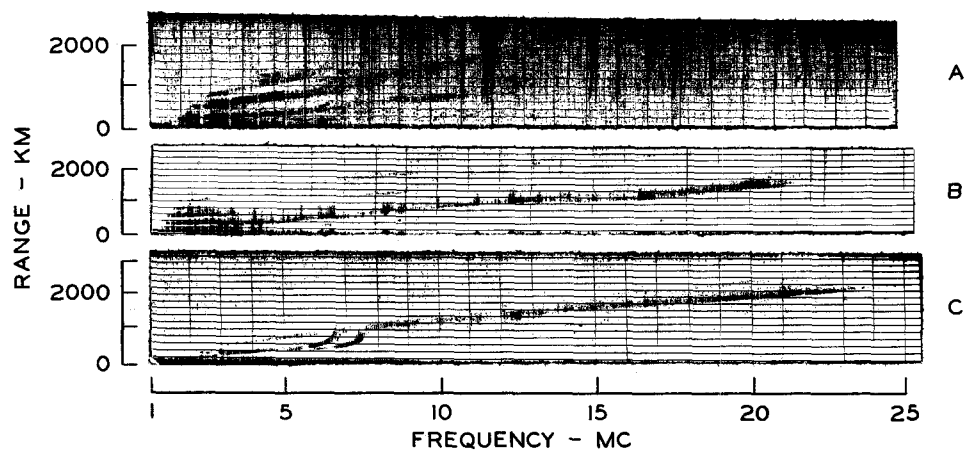


Fig. 6. Particular examples of 1F, 2F, and constant range echoes.

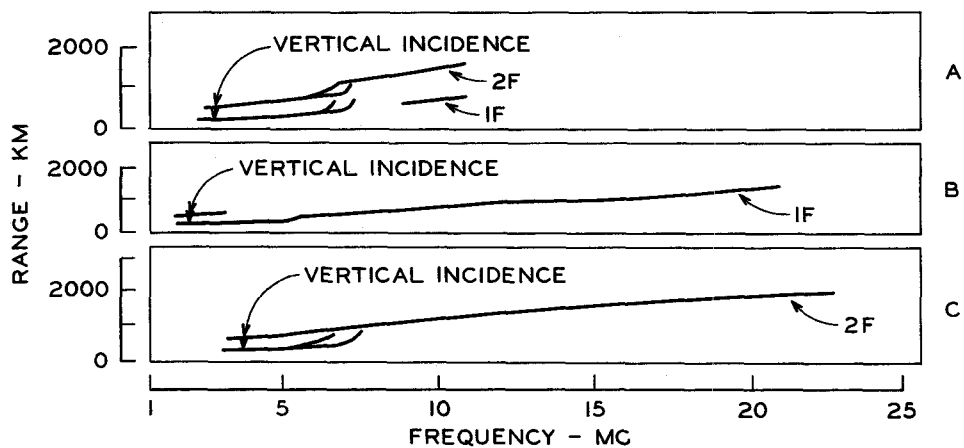


Fig. 7. Line drawing of Figure 6.

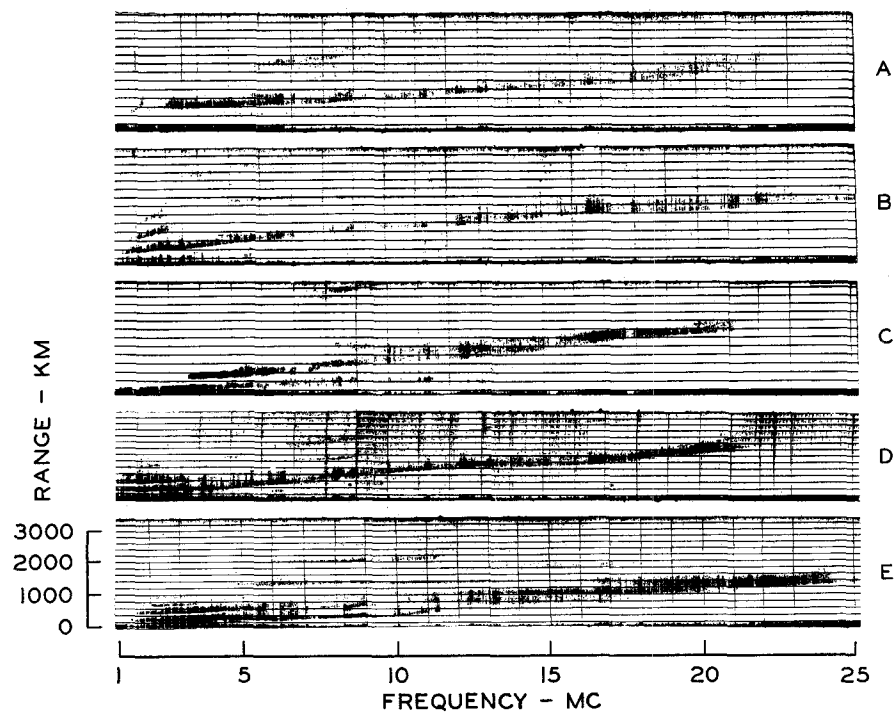


Fig. 8. Typical 1F echoes.

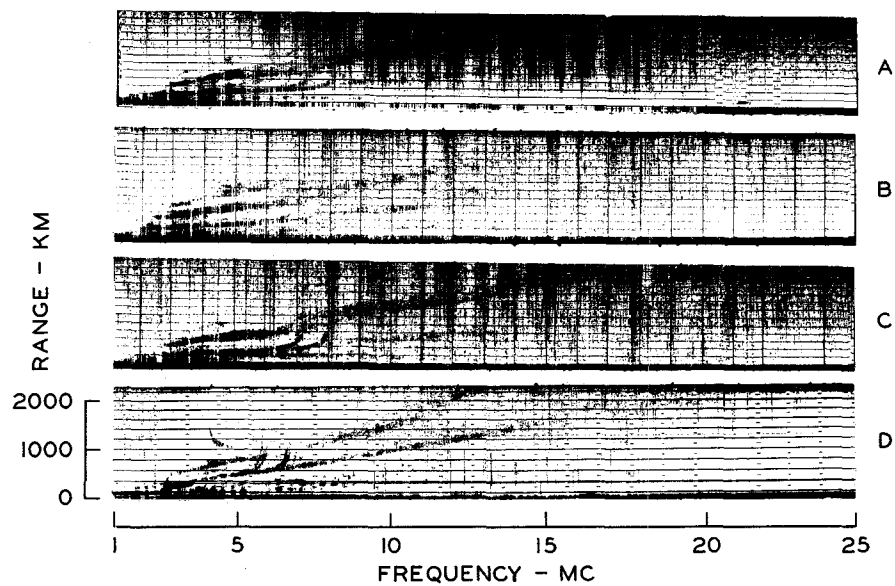


Fig. 9. Simultaneously occurring 1F and 2F echoes.

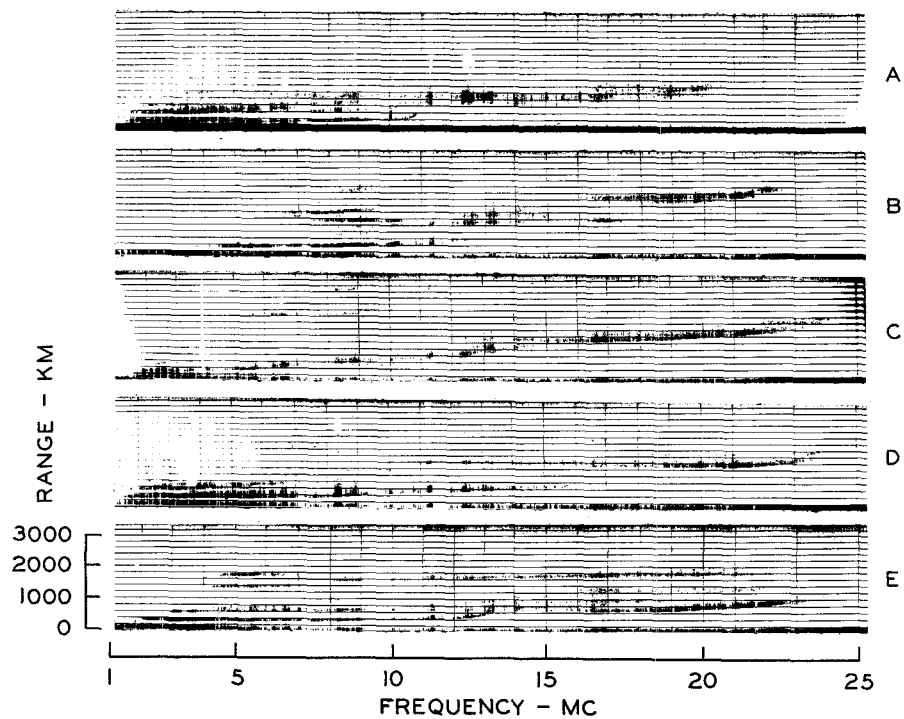


Fig. 10. Constant range echoes.

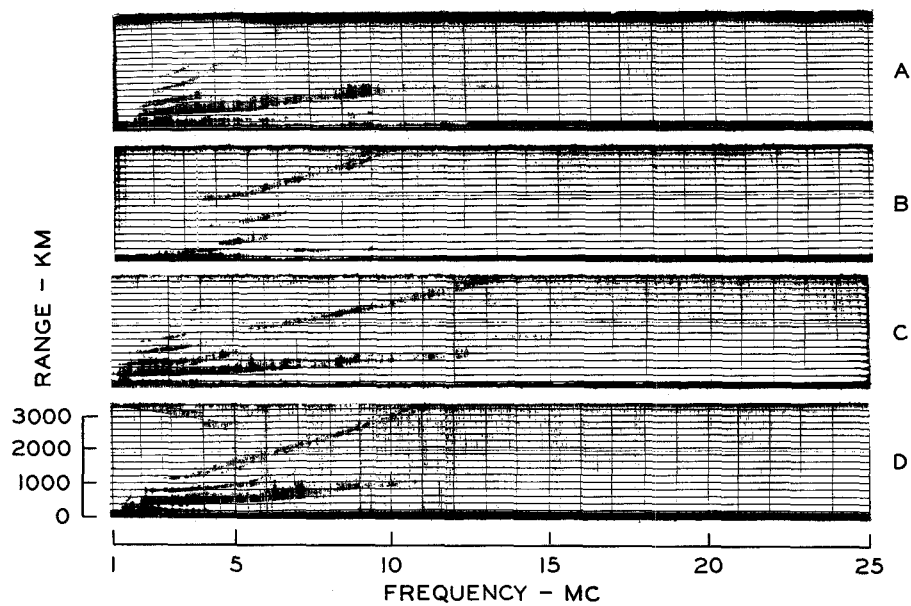


Fig. 11. Possible 3F backscatter echoes.

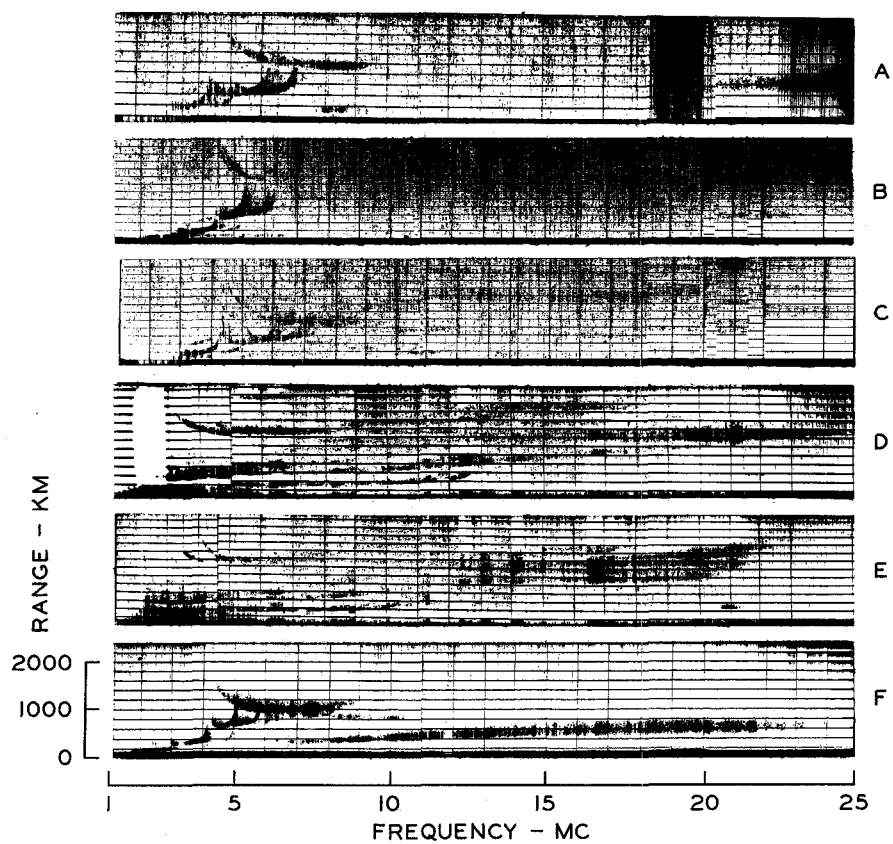


Fig. 12. Cusped, oblique echoes.

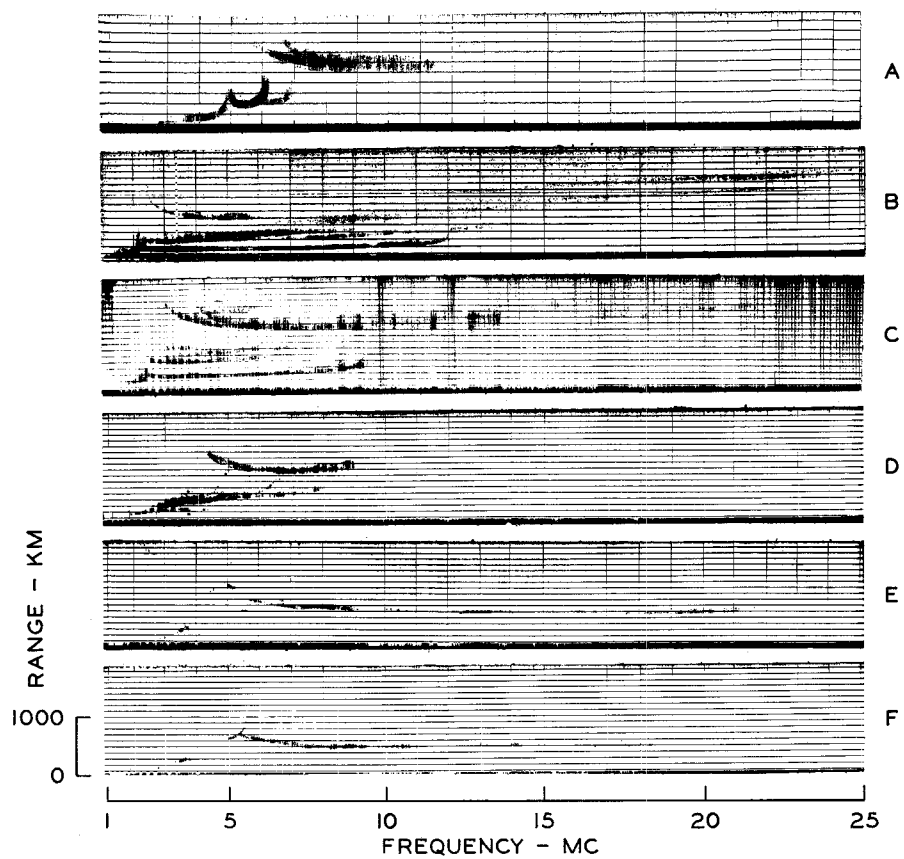


Fig. 13. Cusped, oblique echoes.

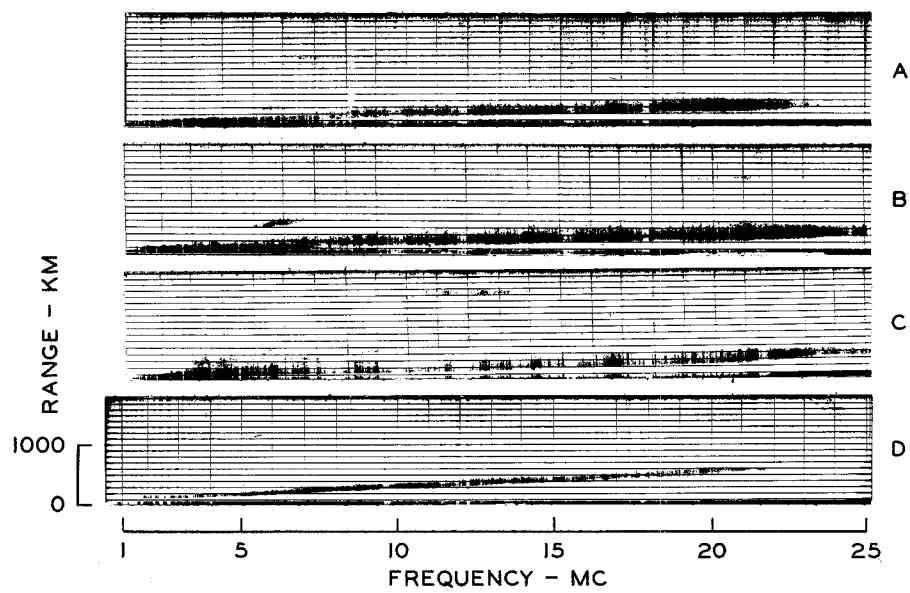


Fig. 14. Slant Es echoes.

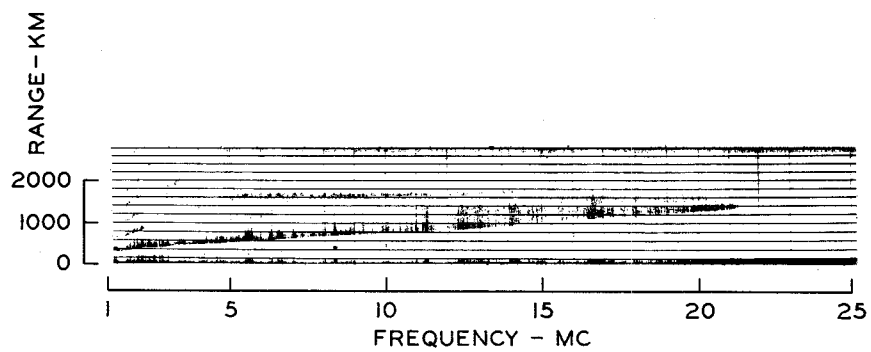


Fig. 15. Typical lF trace.

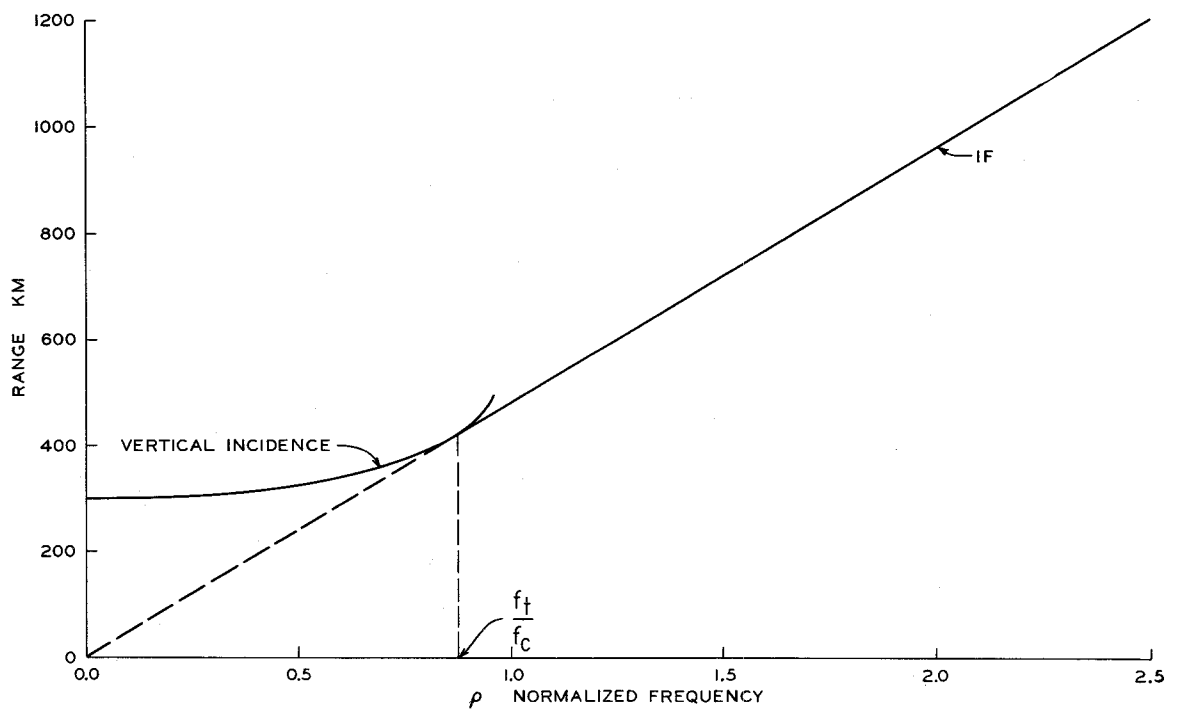


Fig. 16. Calculated lF trace.

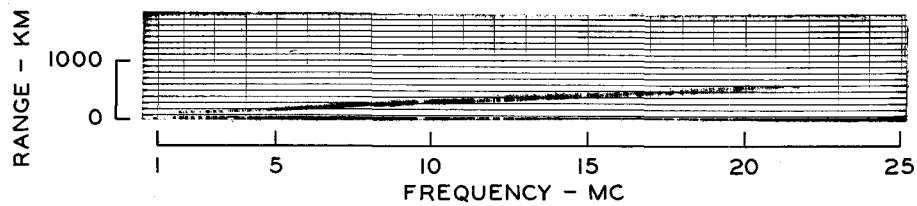


Fig. 17. Example of slant Es.

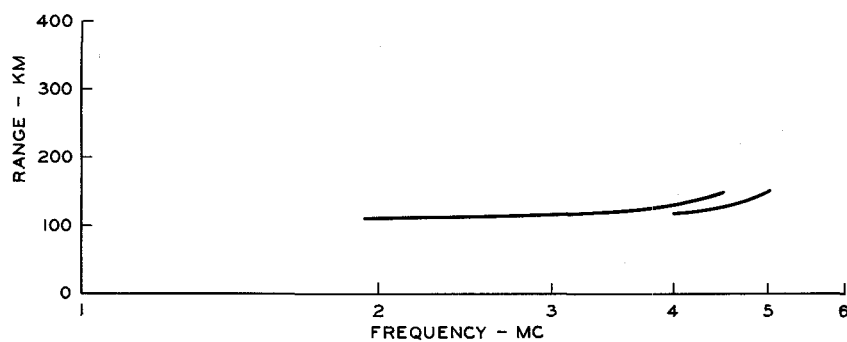


Fig. 18. High resolution vertical incidence trace for Figure 18.

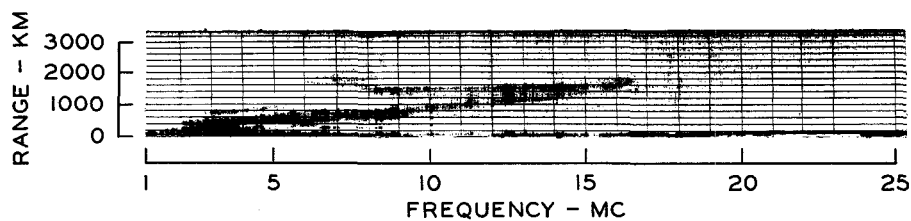


Fig. 19. Typical constant range trace.

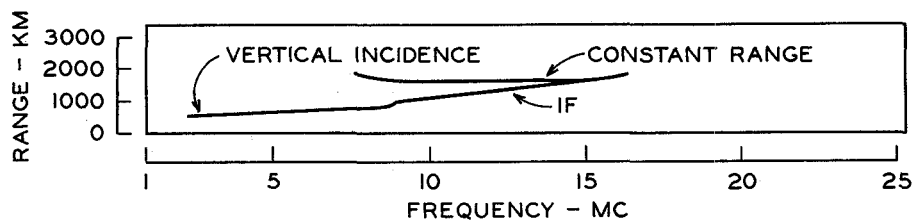


Fig. 20. Line drawing of Figure 19.

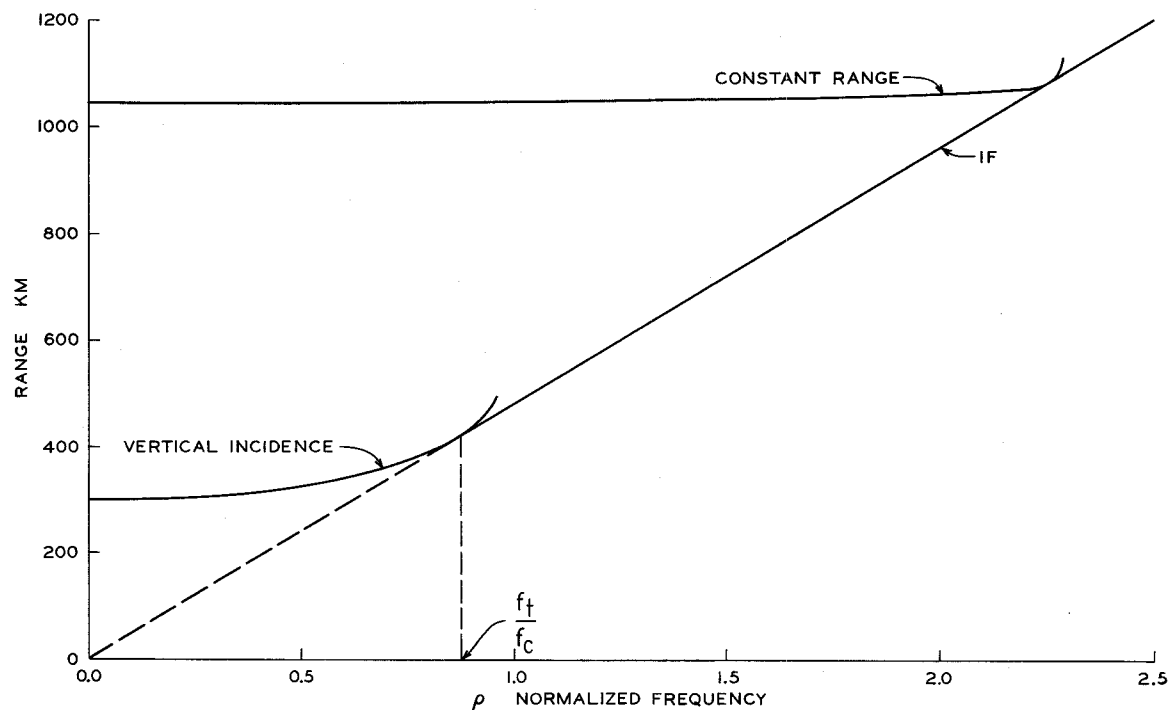


Fig. 21. Calculated 1F and constant range traces.

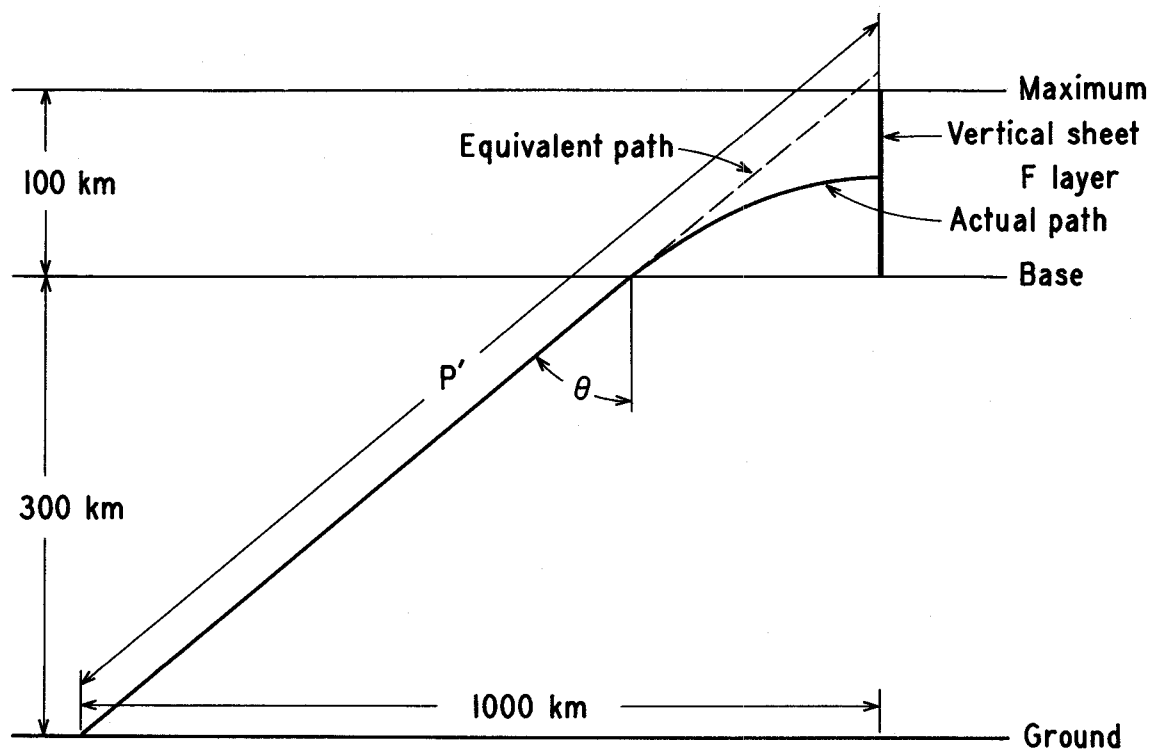


Fig. 22. Geometry for constant range trace calculation.

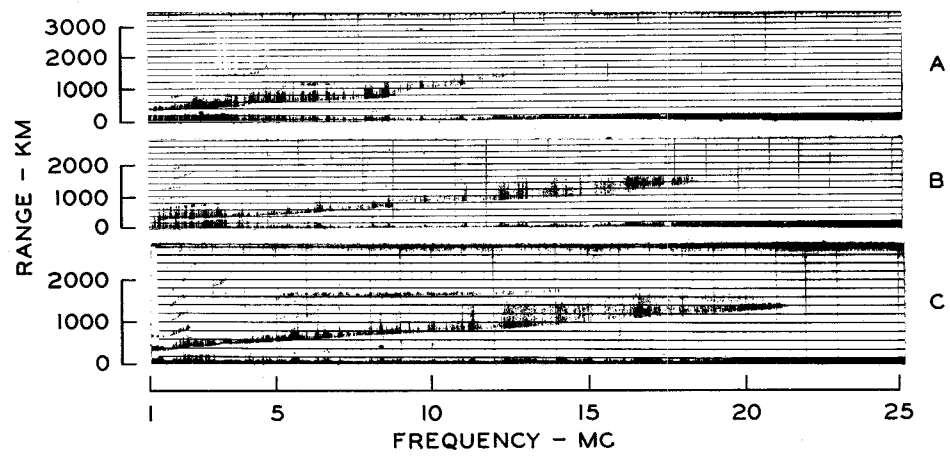


Fig. 23. Typical examples of LF trace.

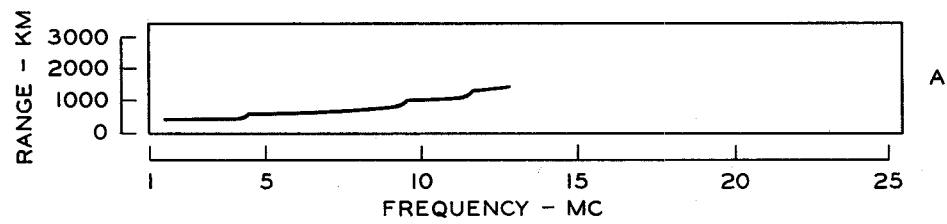


Fig. 24. Line drawing of Figure 23A.

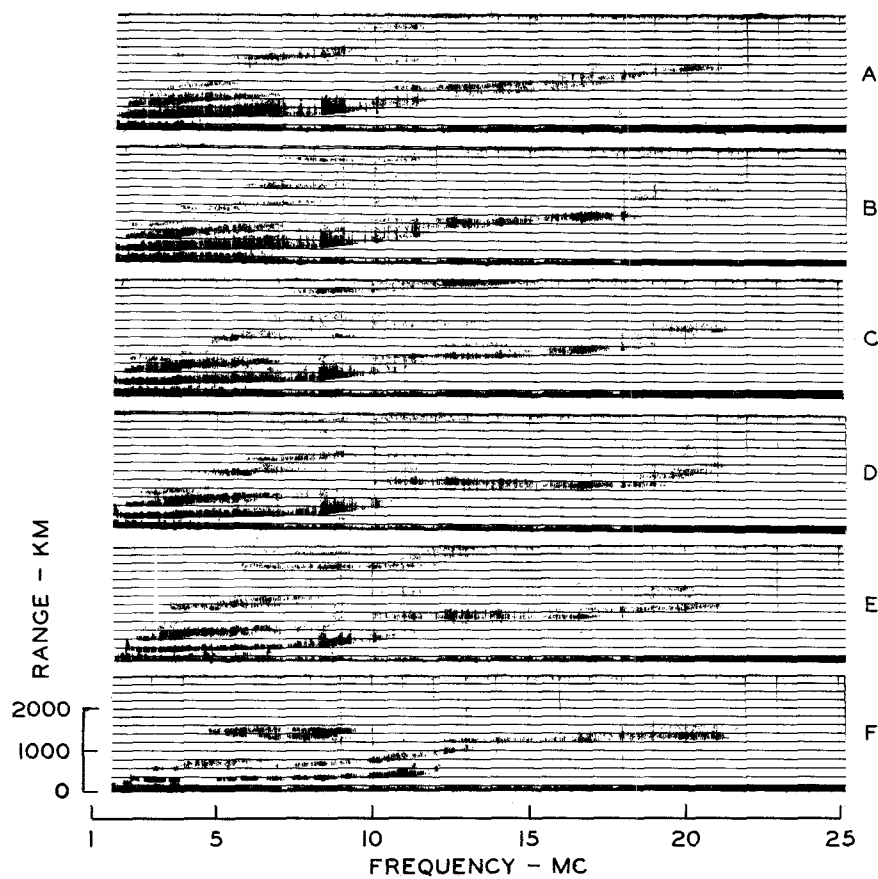


Fig. 25. Morning sequence, 16 November 1958.

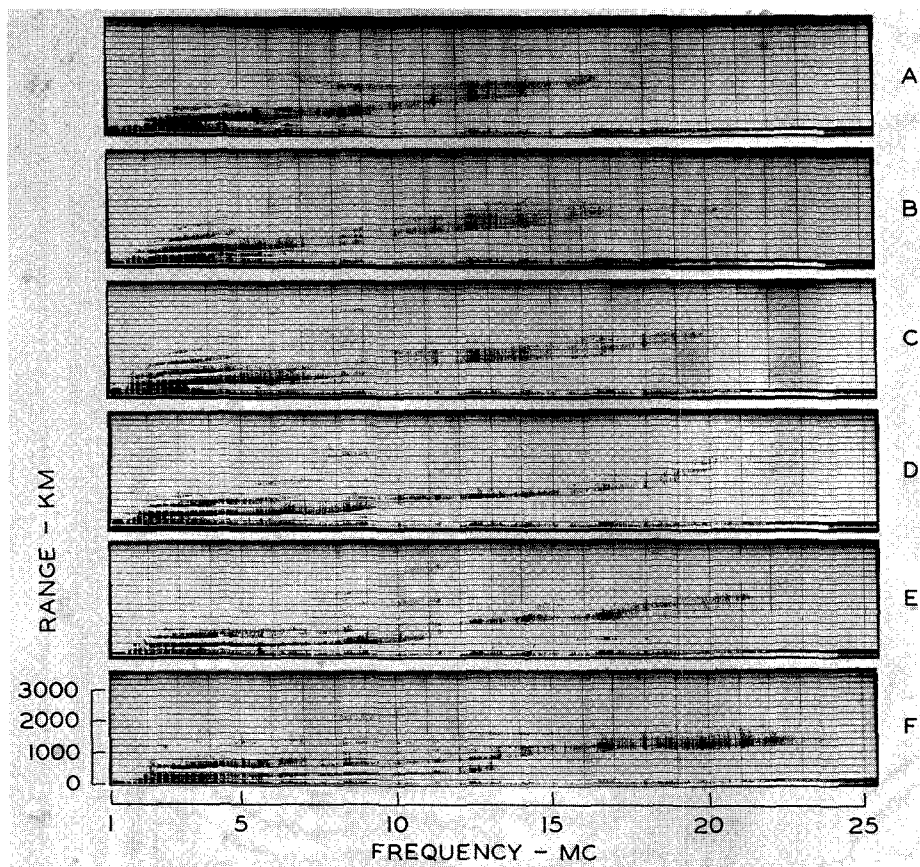


Fig. 26. Morning sequence, 20 December 1958.

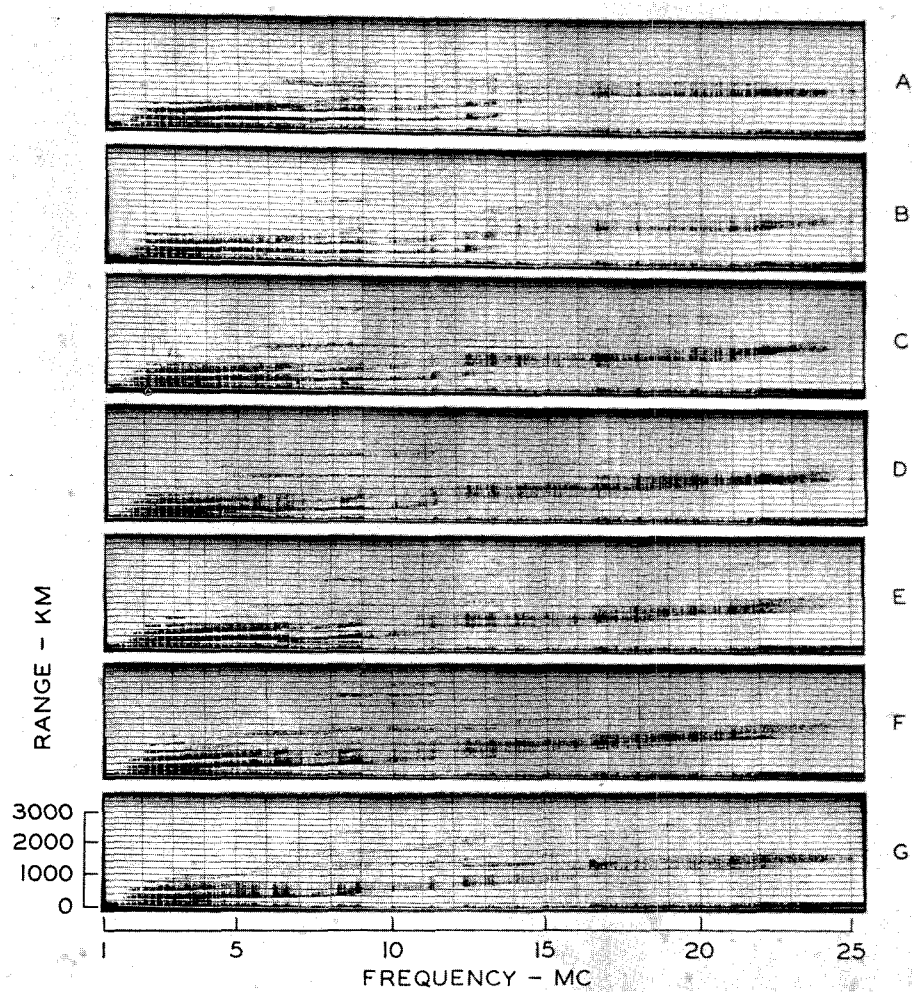


Fig. 27. Afternoon sequence, 20 December 1958.

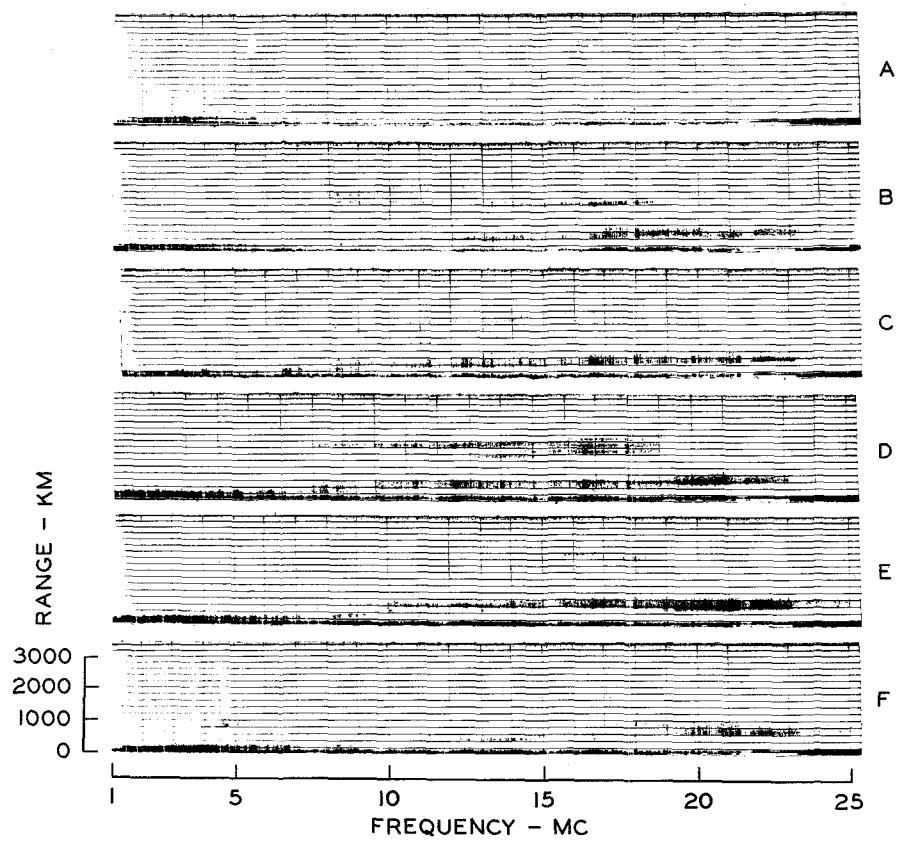


Fig. 23. Slant Es sequence, 23 December 1958.

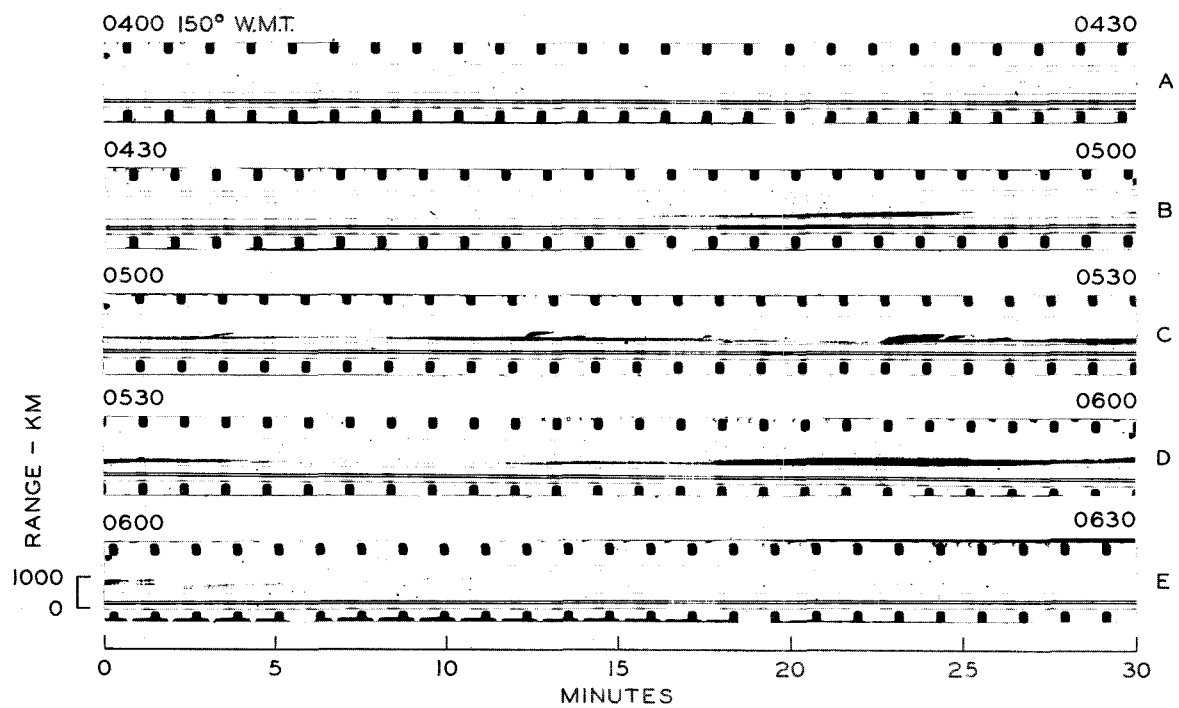


Fig. 29. College 41 Mc/s radar record, 28 December 1958.